Phil. Trans. R. Soc. Lond. B **317**, 365–391 (1987) [365]
Printed in Great Britain

THE INTERPRETATION AND ENVIRONMENTAL SIGNIFICANCE OF A BURIED MIDDLE PLEISTOCENE SOIL NEAR IPSWICH AIRPORT, SUFFOLK, ENGLAND

By R. A. KEMP†

Department of Geography, Birkbeck College, University of London, 7–15 *Gresse Street, London W*1*P* 1*PA, U.K.*

(*Communicated by R. G. West, F.R.S. – Received* 6 *May* 1986)

[Plates 1–10]

CONTENTS

† Present address: Department of Soil Science, Lincoln College, Canterbury, New Zealand.

A buried Middle Pleistocene soil at Ipswich Airport, Suffolk, England, was studied by using macromorphological, textural, mineralogical, chemical and micromorphological techniques. This soil, developed on a low-level terrace surface in the Kesgrave Sands and Gravels, and buried beneath solifluction deposits and the Barham Sands and Gravels, is a composite of the Valley Farm and Barham Soils which have been recognized over wide areas of East Anglia. Clay illuviation, gleying, rubification (haematite formation) and periglacial disruption were the major pedogenic processes active during its formation; mineral weathering and temperate pedoturbation appear to have played only a minor role.

After deposition of the Kesgrave Sands and Gravels and establishment of a stable land surface, clay was translocated from the eluvial horizons into the lower illuvial horizons. Initially, this process consisted solely of fine clay but as the environment deteriorated, coarser and more poorly sorted clay was translocated. Biotic, shrink–swell or frost turbation processes led to localized disruption of some limpid (fine) clay coatings before, or simultaneous with, commencement of this phase of coarser clay illuviation. However, most fragmentation of coatings occurred later when the environment had deteriorated to one characterized by seasonally frozen ground. At this stage, silt grains were translocated and small-scale contraction cracks or microscale cryogenic features (silty clay cappings and duplex textural lamellae features) formed. Further deterioration of climate led to formation of large-scale contraction cracks and soil (or incipient ice) wedges, truncation of the soil and deposition of two solifluction deposits. The older sediment contains components of the eroded eluvial horizons, whereas the other solifluction deposit and the overlying (glacifluvial) Barham Sands and Gravels contain minerals derived from the Anglian ice sheet.

The soil at Ipswich Airport is developed in the Waldringfield Member of the Kesgrave Formation, which is assumed to be of Beestonian age. As the overlying sediments were apparently deposited during the Anglian Stage, it appears that the soil probably formed during the Cromerian and early parts of the Anglian. Such a chronology would not be in dispute with the proposed environmental reconstruction derived largely from pedological evidence, which suggests a simple environmental deterioration from a temperate optimum to that of periglacial conditions. However, much depends on the significance of the first disruption phase. If the fragmentation of limpid clay coatings represents a sharp climatic oscillation, the environmental reconstruction and stratigraphic implications of this soil may be more complex.

1. Introduction

The Valley Farm and Barham Soils are important components of the Middle Pleistocene stratigraphy of southern East Anglia (England). The Valley Farm Soil developed on several low-relief terrace surfaces in the Kesgrave Sands and Gravels, a fluvial sediment deposited in a periglacial environment by a northeastward-flowing proto-Thames (Rose *et al.* 1976). The soil is typically truncated, rubified, mottled and contains considerable amounts of illuvial clay in its remnant illuvial horizons (Kemp 1985*a*). The Barham Soil, which is characterized by periglacial involutions, sand wedges, ice-wedge casts and microscale cryogenic soil features, is sometimes developed in lake sediments but normally occurs superimposed upon the Valley Farm Soil (Rose *et al.* 1985).

Both soils are frequently buried beneath a variety of aeolian, solifluction, glacifluvial or glacial sediments which have all been assigned to the Anglian Stage of the British Quaternary stratigraphy (Rose *et al.* 1976, 1985) (table 1). The buried soils not only represent a break in deposition between these sediments and the underlying Kesgrave Sands and Gravels, but also

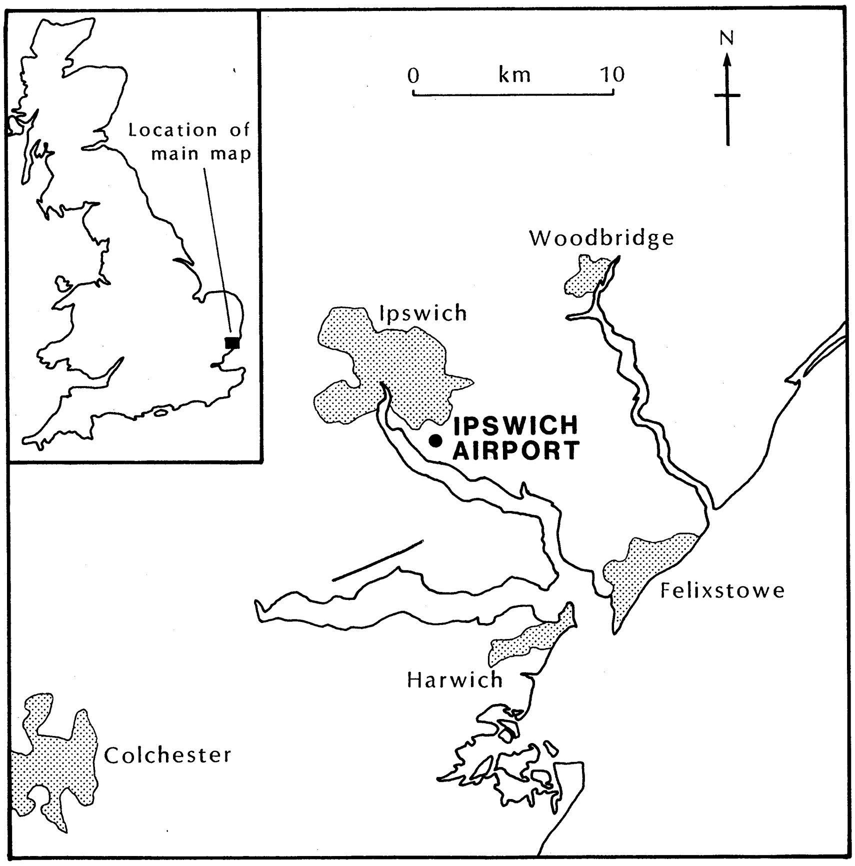

FIGURE 1. Map showing the location of Ipswich Airport.

TABLE 1. THE STRATIGRAPHIC POSITION OF THE VALLEY FARM AND BARHAM SOILS
(After Kemp (1985*a*).)

formation name	soils	environment	probable Stage within the British Quaternary stratigraphy
Lowestoft Till		glacial	
Barham Sands and Gravels		glacifluvial	
Barham Loess	Barham Soil		Anglian
Barham Coversand		periglacial	
Barham Head			
	Valley Farm Soil	temperate	Cromerian
	↓		
Kesgrave Sands and Gravels (lower levels (Hey 1980); Waldringfield Member (Allen 1983))	↓	periglacial	Beestonian
	↓		
	↓	temperate	Pastonian
	?		
Kesgrave Sands and Gravels (upper levels (Hey 1980); Westland Green Member (Allen 1983))		periglacial	Pre-Pastonian

provide valuable information on environmental changes that cannot be obtained from the depositional record.

Hey (1980) subdivided the Kesgrave Formation into a high-level Westland Green Member of possible Pre-Pastonian age and a low-level member of Beestonian age (table 1). A preliminary investigation by Kemp (1985*a*) revealed considerable differences between the Valley Farm Soil on the two respective levels, which could reflect a difference in soil-forming interval. However, he concluded that further sites needed to be studied before it would become necessary to separate the Valley Farm Soil into more than one stratigraphic unit. He proposed that the Valley Farm Soil should for the present be considered as a single soil stratigraphic unit having a minimum age dating to the Cromerian and a maximum age-range equivalent to at least the Pastonian, Beestonian and Cromerian Stages (table 1). Features of the Barham Soil, however, can be more confidently assigned to the Early Anglian (Rose *et al.* 1976, 1985).

The composite soil, referred to by Kemp (1985*a*) as an example of the Valley Farm Soil and superimposed Barham Soils developed on a lower level of the Kesgrave Formation, was at Ipswich Airport, Suffolk (figure 1). It was exposed during the construction of the southeast portion of the Ipswich by-pass during November 1981. The section examined at TM 193410 was within a trench dug several metres below the excavated surface, which was itself approximately 8 m below the present-day land surface. This paper considers the formation and environmental significance of this buried Middle Pleistocene soil.

2. Methods

A drawing was made of the cleared trench section and two profiles were described in detail by using standard Soil Survey terminology (Hodgson 1976). Bulk samples were taken from each horizon of the profiles and undisturbed blocks removed in Kubiena tins from selected horizons for thin-section preparation. The term 'horizon' is used in this study to signify a separable layer, lens or unit of either pedogenic or sedimentary origin.

The bulk samples were air-dried and passed through a 2 mm sieve. All subsequent analyses were done on the smaller than 2 mm fraction of selected samples, unless otherwise specified. Particle size was determined according to the sieving, pipette and centrifuge technique outlined by Avery & Bascomb (1982). Two size-fractions (2.5–3.0 φ† and 4.0–6.0 φ) were separated into heavy and light fractions by using bromoform (specific gravity 2.9). Between 650 and 1100 grains of each light and heavy fraction were immersed in clove oil (refractive index 1.538) and identified with a petrological microscope.

Clay minerals were identified and individual amounts estimated semi-quantitatively by using the procedures and criteria summarized by Avery & Bullock (1977). Several clay fractions were analysed for crystalline iron oxides by differential X-ray diffraction (Brown & Wood 1985). Samples of fractions of less than 2 mm and less than 2 μm were extracted with ammonium oxalate/oxalic acid solution (McKeague & Day 1966) and sodium dithionite/sodium acetate – acetic acid buffer (Avery & Bascomb 1982). Oxalate-extractable iron (Fe_o) and dithionite-extractable iron (Fe_d) were determined colorimetrically according to the method described by Avery & Bascomb (1982). Organic carbon was measured colorimetrically after dichromate oxidation and pH (in 0.01 M $CaCl_2$) was determined with a pH meter (Avery & Bascomb 1982).

† $\varphi = -\log_2$ millimetre transformation.

Thin sections (7.5 cm × 6.0 cm) were prepared from undisturbed blocks with a Crystic polyester resin (Avery & Bascomb 1982), after acetone replacement of the water. The terminology used to describe the thin sections, which is largely based upon that outlined by Bullock *et al.* (1985) with modifications from Kemp (1985*b*), is summarized in Appendix 3.

3. Morphology and particle size

The field description and stratigraphic interpretation of the section from the trench are summarized in figures 2 and 3. Location of the horizons and thin sections from two profiles are also indicated. Particle size data are recorded in table 2 and detailed descriptions of the two profiles are provided in Appendixes 1 and 2.

Four distinct units are present: the Barham Sands and Gravels (BSG), two deposits of a possible solifluction origin (S1 and S2) and a soil developed in the Waldringfield Sands and Gravels (WSG). The WSG are the low-level member of the Kesgrave Formation (Allen 1983).

The uppermost yellow or yellowish brown BSG are up to 9 m thick in adjacent exposures where they extend close to the present-day land surface. They are underlain towards the east–southeast end of the section by a yellowish brown, poorly sorted sandy clay loam (S1, horizon 3 in profile 2). This unit cuts into and partly mixes with an involuted, pale brown, moderately stony loamy sand (S2, horizon 4), which extends across the section immediately beneath the BSG. Both S1 and S2 have relatively high silt contents and are tentatively interpreted as solifluction deposits; S2 has a stone fabric characteristic of such an origin (P. Allen 1981, personal communication).

The upper 15–40 cm of the soil is yellowish brown with a sharp change below to reddish yellow or reddish brown hues. These merge with depth into strong brown and finally brown colours at the base of the section where sandy loam and sand lenses intersperse. The lenses grade upwards into a very slightly stony sand and then into a moderately stony loamy sand. The vertical fining of the less than 2 mm matrix extends to the upper irregular surface of the soil, beneath which the material is a very slightly stony sandy loam.

The textural heterogeneity of the soil is illustrated by the complex depth distribution of sand fraction ratios (table 2). Silt contents in the soil are generally below 2% apart from within the basal fine-textured lenses (1/13) and uppermost horizon (1/6 and 2/6). Maxima clay contents occur just below this concentration of silt at the top of the soil (1/7 and 2/7). Amounts then generally decrease with depth in a pattern independent of changes in the silt : silt + sand ratio. There is a consistent increase in the fine : total clay ratio in both profiles from horizons 4 to 12.

The boundary between the soil and S2 is very irregular with two small wedges and a series of sub-vertical, greyish brown sandy clay fissure zones extending into the upper part of the soil. In profile 1, horizon 4 (S2) dips and merges into a three-pronged wedge of yellowish sand (5) that has an additional complex feeder vein from the top of horizon 6. The latter horizon is upturned at the left-hand margin of the wedge and partly cut out by horizon 4 at the right-hand margin. A simpler wedge of sand cuts into horizons 6/7 and protrudes upwards into horizon 4 of profile 2. Adjacent horizons have sharp boundaries and are upturned at the right-hand margin.

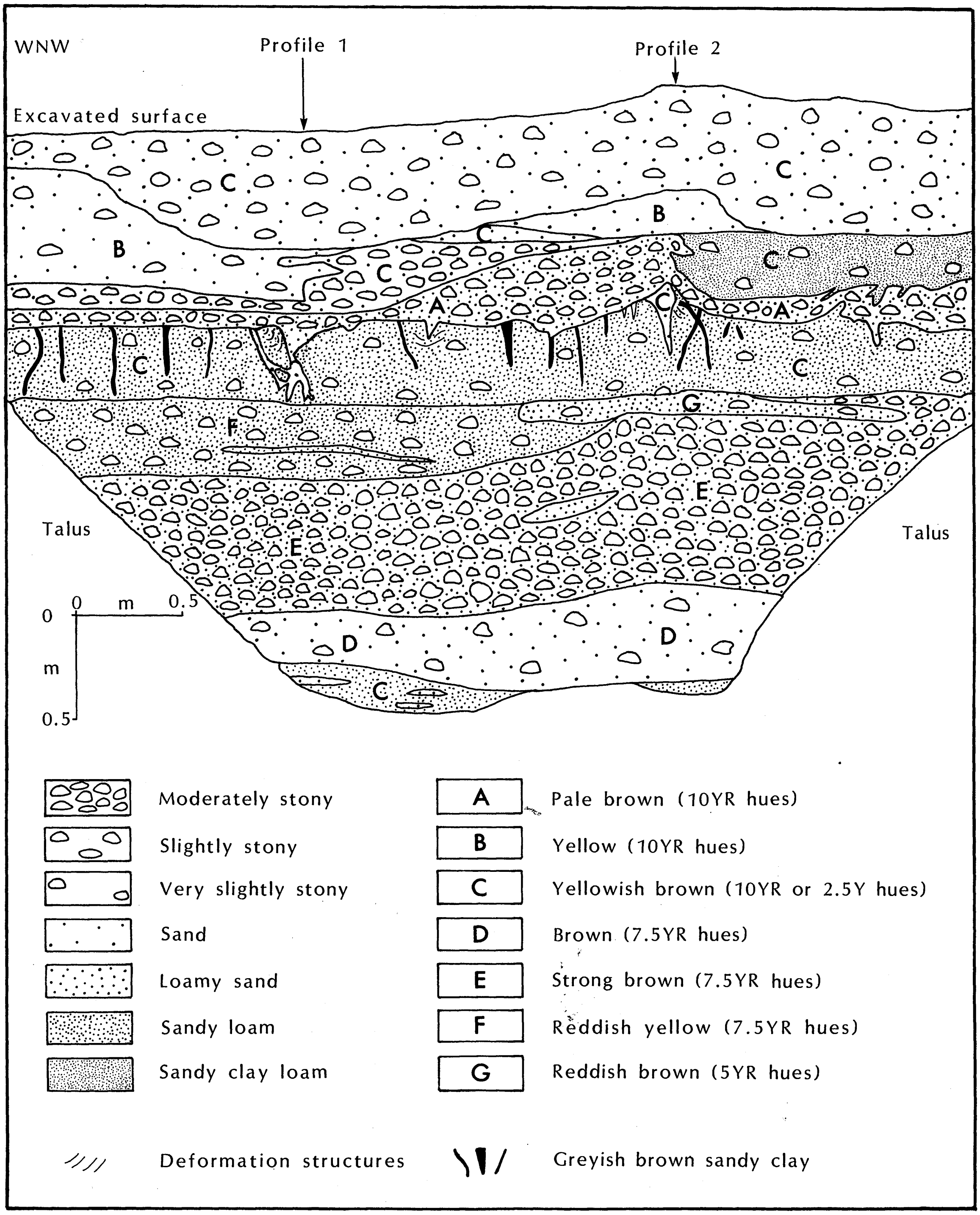

FIGURE 2. Drawing of section from the trench.

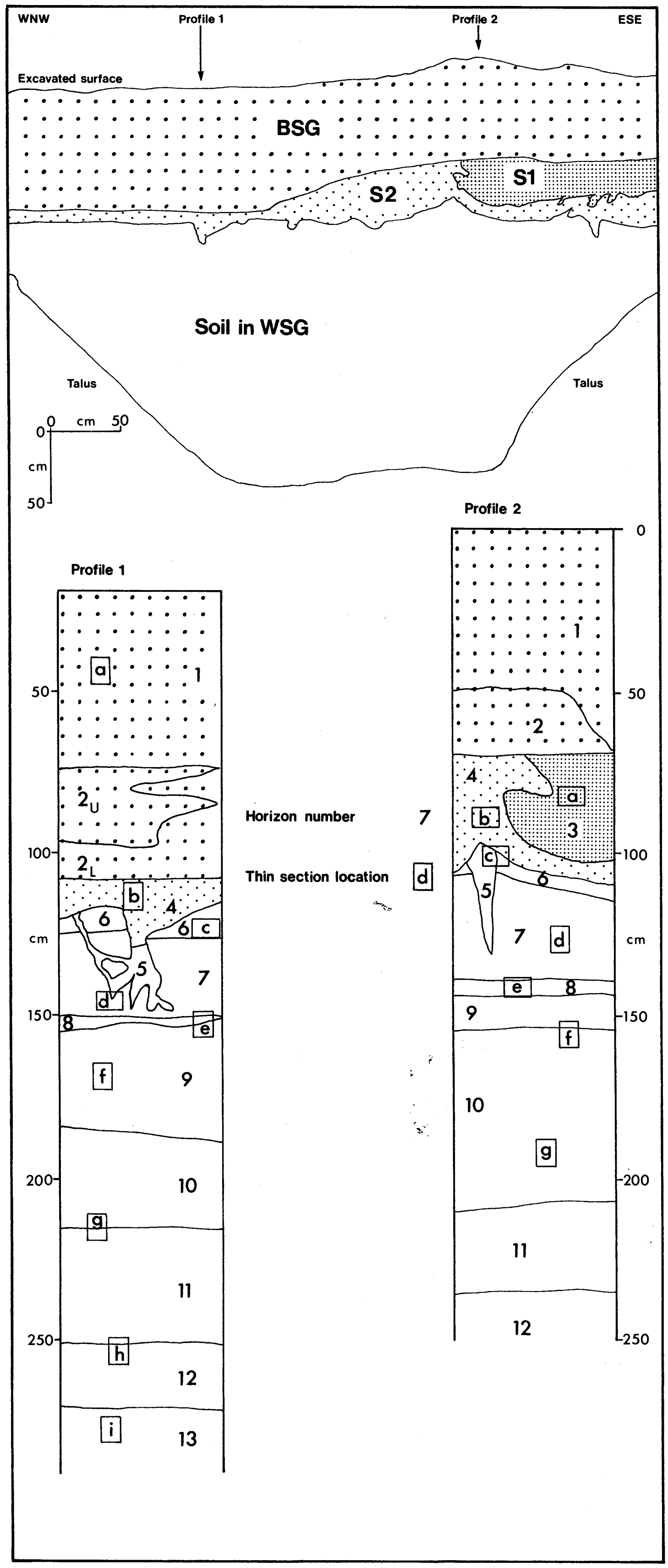

FIGURE 3. Stratigraphic interpretation of the section and details of the profiles.

TABLE 2. PARTICLE SIZE RESULTS FROM BOTH PROFILES AT IPSWICH AIRPORT

profile/ horizon	sand 2–0.063 mm (%)	silt 63–2 μm (%)	clay <2 μm (%)	0–1 φ: 0–2 φ	silt: silt+sand	fine clay: total clay
1/1	94.1	2.3	3.6	0.25	0.02	0.33
$1/2_u$	94.3	1.8	3.9	0.37	0.02	0.28
$1/2_l$	94.0	2.3	3.7	0.45	0.02	0.30
1/4	82.5	13.0	4.5	0.24	0.14	0.22
1/5	91.3	1.7	7.0	0.25	0.02	0.30
1/6	81.0	5.2	13.8	0.09	0.06	0.29
1/7	81.2	1.8	17.0	0.13	0.02	0.30
1/8	86.2	2.1	11.7	0.20	0.02	0.33
1/9	83.7	1.0	15.3	0.33	0.01	0.35
1/10	88.5	1.3	10.2	0.60	0.01	0.45
1/11	90.5	0.6	8.9	0.33	0.01	0.43
1/12	92.4	0.6	7.0	0.34	0.01	0.47
1/13	78.1	8.5	13.4	0.08	0.10	0.31
2/2	97.6	0.9	1.4	0.19	0.01	0.36
2/3	69.5	21.5	9.0	0.17	0.24	0.28
2/4	83.6	12.2	4.2	0.31	0.13	0.21
2/5	89.6	5.2	5.2	0.35	0.05	0.25
2/6	85.5	3.4	11.1	0.12	0.04	0.33
2/7	82.8	1.1	16.1	0.10	0.01	0.35
2/8	84.1	1.3	14.6	0.22	0.02	0.34
2/9	85.9	1.7	12.4	0.29	0.02	0.35
2/10	88.8	0.6	10.6	0.32	0.01	0.40
2/11	89.7	1.7	8.6	0.17	0.02	0.40
2/12	88.8	2.0	9.2	0.67	0.02	0.39

All results refer to the less than 2 mm fraction and are expressed on an oven-dry basis.

4. MINERALOGY

The mineralogy of fine sand (125–180 μm, 2.5–3.0 (φ), coarse silt (16–63 μm, 4.0–6.0 φ) and clay (less than 2 μm, greater than 9.0 (φ) fractions from selected horizons of both profiles are shown in tables 3 and 4.

All horizons have a fine sand mineralogy dominated by quartz with minor amounts of feldspar, quartzite, glauconite and heavy minerals. A considerable proportion of the opaque grains are black under oblique incident light, suggesting appreciable magnetite or ilmenite contents. The non-opaque heavy fractions consist predominantly of the relatively stable minerals zircon and tourmaline with variable quantities of garnet, staurolite, rutile, epidote, zoisite or kyanite. Most grains are partly weathered or at least etched. Zircon: zircon + tourmaline ratios vary markedly from horizon to horizon, confirming the general heterogeneity of the profiles and preventing the establishment of vertical weathering trends. Easily weatherable minerals (collophane and apatite) occur in small quantities only in the BSG and S1 units. These horizons (1/1, $1/2_u$, $1/2_l$ and 2/3) differ also in having higher heavy mineral contents and relatively large quantities of garnet resulting in garnet–tourmaline heavy mineral assemblages.

The sand fraction from horizon 13 at the base of profile 1 contains significant amounts of phyllosilicates (biotite or chlorite or both), minerals that are rare or absent elsewhere except within the silt-size fractions of S2 (1/4). The silt mineralogy of the soil and S2 is generally

TABLE 3. SILT AND SAND MINERALOGY OF SELECTED HORIZONS FROM BOTH PROFILES AT IPSWICH AIRPORT

	profile/horizon														
	1/1	$1/2_u$	$1/2_l$	1/4	1/5	1/6	1/7	1/9	1/13	2/3	2/4	2/5	1/4†	1/6†	1/13†
% heavy minerals	1.2	2.1	3.3	0.2	0.2	0.7	0.8	0.9	0.2	0.8	0.3	0.3	1.1	0.2	0.3
% non-opaques in heavy fraction	10.7	14.6	18.5	44.2	34.4	33.9	29.0	44.5	43.9	15.5	28.4	32.7	60.8	41.1	35.2
% magnetite‡ in opaques	n.d.	n.d.	n.d.	42.1	38.9	n.d.	n.d.	n.d.	n.d.	n.d.	n.d.	n.d.	n.d.	n.d.	n.d.
tourmaline	204	101	152	439	422	294	394	185	333	292	443	140	43	105	49
zircon	88	56	86	173	175	257	218	367	26	68	157	363	382	384	599
garnet	339	487	416	130	121	132	77	181	86	291	131	131	105	55	21
rutile	32	53	27	57	58	89	67	86	37	19	56	93	46	50	79
epidote	58	62	52	9	26	10	17	27	67	54	17	27	110	210	112
zoisite	21	18	22	5	3	5	8	4	34	22	5	—	74	84	33
staurolite	72	99	74	118	128	143	115	89	95	93	129	126	23	10	7
kyanite	35	39	29	44	52	59	79	43	50	28	41	99	34	23	24
andalusite	39	15	6	12	5	6	18	8	41	16	9	16	14	2	—
hornblende	79	44	89	11	10	3	4	10	72	64	8	5	46	8	2
tremolite	5	—	1	2	—	1	3	—	9	3	2	—	18	6	2
augite	—	8	1	—	—	—	—	—	—	—	—	—	4	—	6
collophane	19	15	27	—	—	—	—	—	—	39	—	—	—	—	—
apatite	4	2	—	—	—	—	—	—	—	2	—	—	—	—	—
mica	5	—	17	—	—	—	—	—	148	3	—	—	32	4	19
spinel	—	—	—	—	—	1	—	—	2	—	2	—	—	—	4
sphene	—	1	1	—	—	—	—	—	—	—	—	—	7	—	3
sillimanite	—	—	—	—	—	—	—	—	—	4	—	—	7	2	—
brookite	—	—	—	—	—	—	—	—	—	2	—	—	21	19	16
anatase	—	—	—	—	—	—	—	—	—	—	—	—	34	38	24
z:(z+t)	0.30	0.36	0.36	0.28	0.29	0.47	0.36	0.67	0.07	0.19	0.26	0.72	0.90	0.79	0.92
quartz	939	922	920	896	930	899	928	n.d.	892	889	938	918	832	894	901
alkali feldspar	46	65	62	77	42	69	45	n.d.	79	92	41	62	90	99	84
chert	4	6	15	2	14	22	9	n.d.	9	10	11	16	22	—	7
quartzite	4	5	3	13	11	7	10	n.d.	8	7	10	1	—	—	—
glauconite	6	2	—	12	3	3	8	n.d.	4	2	—	3	—	2	3
mica	1	—	—	—	—	—	—	n.d.	8	—	—	—	56	5	3
plagioclase	—	—	—	—	—	—	—	n.d.	—	—	—	—	—	—	2

Size fractions used are 2.5–3.0 φ, apart from † which are 4.0–6.0 φ. Except where stated otherwise, the amounts refer to parts per thousand of the total identifiable light and non-opaque heavy fractions. z = zircon, t = tourmaline, ‡ = magnitite or ilmenite or both (black under oblique incident light). n.d., No determination; —, negligible quantities.

TABLE 4. CLAY AND IRON OXIDE MINERALOGY OF SELECTED HORIZONS FROM BOTH PROFILES AT IPSWICH AIRPORT

profile/horizon	mica	kaolin	interstratified smectite	haematite (%)	goethite (%)
1/1	d	b	e	n.d.	n.d.
1/4	a	b	f†	n.d.	n.d.
1/6	a	b	f†	n.d.	n.d.
1/7	a	b	f	n.d.	n.d.
1/9	a	b	f	0.9	19.3
1/11	a	b	f	n.d.	n.d.
1/13	e	b	d	n.d.	n.d.
2/9	a	b	f	1.1	29.0

a, less than 5%; b, 5–15%; c, 15–30%; d, 30–50%; e, 50–70%; f, >70%; † signifies containing discrete vermiculite component. n.d., No determination.

Haematite and goethite contents are based upon a combination of chemical (Fe_o, Fe_d) and X-ray data (Brown & Wood 1985).

similar to that of the coarser fraction, though relative abundances differ. Easily weatherable minerals, such as collophane or apatite, are absent.

A randomly interstratified smectite, which contains a discrete vermiculite component in 1/4 and 1/6, is the dominant clay mineral in most horizons sampled. Only subsidiary amounts of kaolinite and trace quantities of mica are present. Mica, however, becomes considerably more abundant at the expense of the interstratified smectite in the BSG (1/1) and fine-textured lenses at the base of profile 1 (1/13).

Haematite makes up 0.9% and 1.1% respectively of the clay-size fractions of the two reddest horizons in the soil (1/9 and 2/9).

5. CHEMISTRY

Extractable-iron contents and pH values for selected horizons from both profiles are shown in table 5. Oxalate-extractable iron (Fe_o) is normally taken to approximate the iron present in amorphous oxides (McKeague & Day 1966), although ferrihydrite also dissolves in the extractant (Schwertmann & Taylor 1977) and magnetite, ilmenite and lepidocrocite may be partly soluble (Schwertmann & Taylor 1977; Rhoton *et al.* 1981). Dithionite-extractable iron (Fe_d) approximates the iron present in all amorphous and crystalline oxides with the exception of magnetite (Rhoton *et al.* 1981). Despite limitations to the exact characterization of extracted forms, Fe_o and Fe_d values are frequently expressed in terms of an activity ratio (Fe_o:Fe_d), which is used to indicate the relative ageing or crystallinity of free iron oxides (Blume & Schwertmann 1969).

Fe_d contents of the less than 2 mm fraction vary considerably, ranging from 0.08% in S2 (1/4) to 1.90% at depth within the soil (2/9). The lower Fe_o contents (0.07–1.00%) display a similar irregular trend. Large quantities of iron oxides are present in the clay-size fractions of 1/9 and 2/9 (13.30% and 20.83% Fe_d respectively). The activity ratios are considerably lower than for the corresponding less than 2 mm fractions.

The pH values in profile 1 vary between 4.9 and 5.4, the two extreme values occurring in horizons 1 and 4 respectively. No measurable organic matter is present in any of the horizons, or in the subsamples of the greyish brown fissure-shaped zones in 2/7.

TABLE 5. EXTRACTABLE-IRON CONTENTS AND pH OF SELECTED HORIZONS FROM BOTH PROFILES AT IPSWICH AIRPORT

profile/horizon	pH ($CaCl_2$)	Fe_o (%)	Fe_d (%)	$Fe_o:Fe_d$
1/1	4.9	0.17	0.62	0.27
1/4	5.4	0.07	0.08	0.88
1/5	5.3	n.d.	n.d.	n.d.
1/6	n.d.	0.22	0.40	0.55
1/7	5.2	0.24	0.74	0.32
1/9	5.2	0.46	1.10	0.42
1/10	5.2	0.19	0.30	0.63
1/11	5.3	0.15	0.57	0.26
1/12	5.2	n.d.	n.d.	n.d.
1/13	5.3	0.08	0.16	0.50
2/9	n.d.	1.00	1.90	0.53
1/9†	n.d.	0.53	13.30	0.03
2/9†	n.d.	1.46	20.83	0.07

Analysis performed on the less than 2 mm fraction except †, which refer to the less than 2 μm fraction. All results are expressed on an oven-dry basis. n.d., No determination.

6. MICROMORPHOLOGY

(a) *Introduction and terminology*

A 'concentration feature' is defined in this study as a discrete fabric unit distinguished from adjacent material by a difference in concentration in one or more components. The term is restricted to units having at least a potential pedogenic origin: coatings of all compositions are included, but obvious sedimentary bedding associated with variable sorting or graded bedding is considered as 'groundmass' (Appendix 3). Areal cover of clay concentration features (CCF, expressed as a percentage) (determined on a void- and gravel-free basis: Murphy & Kemp (1984)) is therefore broadly equivalent to illuvial clay content in soils, though CCF does not differentiate between clay coatings produced by pedogenic and non-pedogenic processes (Brewer 1972; Walker *et al.* 1978).

The location of the thin sections referred to in the subsequent discussion are shown in figure 3. The number prefix refers to the appropriate profile, e.g. 2b: thin section b from profile 2.

(b) *Thin-section descriptions*

The BSG (thin section 1a) consist of loose sand grains with a few thin, patchy, flecked continuous, speckled clay infillings of the indentations. S1 (thin section 2a) has a poorly sorted, yellowish brown groundmass with no concentration features, whereas S2 (thin sections 1b and 2b) is coarser textured with common coarse sand grains loose or embedded within aggregates of grey, stipple-speckled finer material. In parts of thin sections 1b and 2c, towards the base of S2, the embedded grains have thin yellowish brown, flecked continuous, speckled to impure clay coatings (figure 4, plate 1).

The parts of thin sections 1d and 2c within the wedges consist of loose sand grains that are uncoated or have thin orange–brown, flecked continuous, impure clay coatings. Between the grains are a very few rounded, fragmented impure clay coatings.

Most of the less than 10 μm fraction in thin sections from the soil occurs as textural concentration features. In thin sections 1c and 2c (CCF = 20–30%) from the uppermost horizons of the soil, the sand grains have orange–brown, flecked continuous, speckled, impure or silty clay coatings. The grains are either loosely distributed or embedded within localized clusters of silt-size mineral grains, rounded fragmented impure clay coatings and rare fragmented limpid clay coatings (figure 5, plate 2). A very few of the sand grains have thin limpid clay predating the coarser clay coatings. More angular fragmented coatings occur between the loose (coated) grains or adjacent to the very few fractured bridge coatings in zones where silt-size mineral grains are absent. A few sub-vertically oriented prolate coarser sand grains have silty clay cappings (figure 6, plate 3), whereas one chert clast in thin section 1c is fractured into conjoinable fragments (figure 7, plate 4). The clay coatings are considerably thinner along the fracture surfaces than upon the original clast surface.

CCF reaches a maximum of 35% in thin section 2d from horizon 7. All of the textural concentration features are in the form of thick yellowish brown, flecked continuous, fractured or fragmented, speckled to impure clay, grain and bridge coatings. The greyish brown, fissure-shaped zones consist of complete fragmented, linear infillings of isolated sand grains within identical material to that comprising the rest of the textural concentration features. Some glauconite grains in this and other thin sections from the soil are fractured and fragmented (figure 8, plate 5).

Thin section 1c contains two linear features, which are up to 5 mm in length and composed of two sub-horizontal lamellae. The lower (50–300 μm thick) has a few dispersed fragmented clay coatings embedded within an orange–brown, speckled to impure clay which has an unistrial b-fabric parallel to the lineation. This lamella has a distinct, clear boundary to the loose or bridged coated grains below. The upper lamella (300–800 μm thick) consists of uncoated or partly coated sand grains that contrast markedly with the more densely packed and thickly coated sand grains above. Duplex textural lamellae feature is introduced as a purely descriptive term to characterize this concentration feature (Kemp 1985*b*), whose dimensions vary considerably in other thin sections, sometimes being over 3 cm long and up to 2 mm thick.

The lamellae are not so clearly defined in thin section 2e from horizon 8, as the sand grains frequently touch and partly extend into the upper parts of the lower lamellae which tend to have less marked unistrial orientations (figure 9, plate 6). Consequently, the features are differentiated by the prefix 'a'. These duplex textural a-features often coincide with horizontally sorted sand lenses, producing a distinct platy structure (figure 10, plate 7). Between the duplex textural lamellae a-features, the sand grains have very rare orange–brown, continuous limpid clay coatings and later more frequent flecked continuous, speckled to impure clay coatings. The latter extend into fractured bridge coatings or infillings.

This coating stratigraphy becomes more widespread lower down in the soil within thin sections 1e, 1f, 2e and 2f (CCF = 25%). Yellowish brown, continuous, limpid clay coatings, which extend around and bridge the sand grains, are clearly postdated by microlaminated, orange–brown to yellowish brown, continuous to flecked continuous, speckled to impure clay, grain or bridge coatings and partial infillings (figure 11, plate 8). A few large fragmented, irregular units of these compound coatings occur adjacent to the coated grains, whereas a very few fragmented limpid clay coatings are loose or embedded within the second phase coatings (figure 12, plate 9). Many of the compound coatings have brown, isotropic laminations, or strongly impregnated, diffuse ferruginous segregations and halo nodules superimposed across the microlaminations.

CCF decreases to less than 20% in horizons 10, 11 and 12 of both profiles (thin sections 1g, 1h and 2g). The sand grains are coated by continuous to flecked continuous, limpid to speckled clay coatings with numerous isotropic microlaminations and ferruginous segregations. The few bridge coatings are commonly fractured and angular fragmented clay coatings are occasionally present between the grains.

CCF is less than 2% in thin section 1i (horizon 13) where only a few of the sand grains have thin, flecked continuous, speckled clay coatings. Thick silty clay, micaceous aggregates (0.1–5.5 mm × 0.2–5.0 mm) are randomly dispersed among the grains (figure 13, plate 10). These aggregates are predominantly grey with a few brown diffuse segregations and common yellowish brown hypocoatings around vughs or planar voids. Prolate grains and planar voids are frequently aligned parallel to the direction of the unistrial b-fabric and long axis of the aggregates. The upper or lower surface of some of the aggregates have thin continuous, limpid to speckled clay coatings.

7. Genesis and environmental significance of the buried soil

(a) *Clay illuviation*

The clay present within the discontinuous, fine textured lenses towards the base of the buried soil is largely sedimentary in origin, reflecting periodic decreases in energy within the depositional environment. Some clay concentrations in both the BSG and WSG may be derived from earlier pedogenic cycles or reflect some form of post-depositional infiltration of clay-size particles into the large packing voids of the sandy sediments at low water flow stages (Walker *et al.* 1978). However, most of the clay concentration features in the buried soil occur in complex associations that are unlikely to have been produced by such processes. These features are attributed to *in situ* pedogenic clay illuviation.

A textural fining of the illuvial clay with depth is indicated by the thin sections, which show that the clay concentration features are predominantly speckled to impure at the top of the soil and more limpid to speckled towards the base. This phenomenon is well established in soils and results from the greater mobility of fine relative to coarse clay (Torrent *et al.* 1980). A simple, one-phase vertical sorting mechanism, however, is not sufficient to account for the complex distribution and association of illuvial features in the soil profiles. Two major phases of clay illuviation are proposed on the basis of superposition of components within compound coatings. The initial phase, during which mainly fine clay was translocated, resulted in non-laminated and microlaminated, continuous limpid or speckled clay, grain and bridge coatings. The second phase consisted of translocation of a more poorly sorted clay with flecked continuous, speckled to impure clay coatings and infillings accumulating at the top of the Bt horizons, the more mobile finer clay being moved further down the profiles to produce microlaminated, limpid and speckled clay coatings. These clearly defined illuvial phases are largely responsible for the increase in fine to total clay ratios with soil depth.

The distinction between the two phases is not always possible in lower parts of the profiles because of the similarity in properties of the respective features. However, towards the top of the soil, compound coatings consist of clearly defined limpid units postdated by more poorly oriented, speckled to impure clay material. Indeed at the very top of the truncated soil, virtually all the illuvial clay has the composition typical of the second phase, suggesting that the earliest phase of illuviation was initiated lower down the profile and that the later phase resulted in an effective upward growth of the Bt horizons.

The interpretation of different illuvial textural concentrations is not straightforward as a variety of factors may determine the size of material translocated. Federoff & Goldberg (1982) related the textural differences between juxtapositional coarse and fine clay coatings in a buried soil from the Paris Basin to a change in environmental conditions, the coarser clay coatings indicating a more aggressive eluviation phase occurring under a cold, moist environment before the establishment of a more temperate climate associated with an interglacial. A similar explanation may account for the two illuvial phases at Ipswich Airport, although in this case the change would have been from a temperate to a cooler environment.

(*b*) *Disruption of clay coatings*

The occurrence of fragmented limpid clay coatings, locally embedded within the coarser clay coatings, may substantiate the concept of an environmental deterioration. Disruption of clay coatings by frost action is known to take place in cold environments (Van Vliet-Lanoe 1985), and presumably could have occurred intermittently during the phase of coarser clay illuviation. Some workers have interpreted fragmented coatings ('papules': Brewer (1976)) in terms of unstable phases of mass-wasting (Mucher *et al.* 1972; Bullock & Murphy 1979) or cryoturbation (Bullock & Murphy 1979; Chartres 1980) at times distinct from the phases of illuviation. The *in situ* disruption of limpid clay coatings at Ipswich Airport, demonstrated by the close association of both undisturbed and fragmented features in the same zones, precludes the possibility of the transported origin, although a discrete cryoturbation phase cannot be discounted. Other interpretations of fragmented coatings have centred on more traditional pedoturbation processes, involving either floral and faunal disruption (Bouma *et al.* 1968) or shrink–swell movements due to wetting and drying stresses (Castellet & FitzPatrick 1974). These may provide equally adequate explanations for the localized disruption of the limpid clay coatings.

The extensive fracturing and fragmentation of the second phase clay coatings can be more confidently ascribed to cold climate disruptive processes as there are many associated features indicative of such an environment being present. Thin section 1c contains one chert clast that has been fractured into conjoinable fragments, a feature commonly attributed to frost shattering during freeze–thaw cycles (FitzPatrick 1974). The thin impure clay coatings on the fracture surfaces, as compared with the thicker one around the original clast surface, suggest that the shattering occurred during, rather than before or after, the second illuvial phase.

The fine-textured lenses at the base of the soil are severely fragmented. The partial mixing of the resultant aggregates with the coated sand grains suggests that the disruption postdated clay illuviation, and is presumably a further consequence of freeze–thaw activity.

(*c*) *Formation of duplex textural lamellae features*

The duplex textural lamellae features, present in a number of the upper horizons of the soil, resemble other banded features described in soils from temperate and more northern latitudes (McMillan & Mitchell 1953; Dumanski 1964; Dumanski & St. Arnaud 1966; Romans *et al.* 1966, 1980; McKeague *et al.* 1974; Romans & Robertson 1974; Pawluk & Brewer 1975; Van Vliet-Lanoe 1976, 1982; Harris & Ellis 1980; Mermut & St. Arnaud 1981; Harris 1985). Banded fabrics in eluvial horizons in Saskatchewan were first described by McMillan & Mitchell (1953) and later considered in more detail by Dumanski & St. Arnaud (1966) and McKeague *et al.* (1974). Although their genesis was not satisfactorily established, Dumanski

(1964) was able to produce similar fabrics, consisting of 'more or less horizontal, lenticular or curved planar voids separating platy and elliptical units in which plasma is concentrated in the upper part' (McKeague *et al.* 1974, p. 87), by repeatedly freezing and thawing eluvial soil material.

Less well-developed banded fabrics were reported from Arctic Canada by Pawluk & Brewer (1975), and Mermut & St. Arnaud (1981) described similar but smaller 'microband fabrics' in subsoil horizons in central Saskatchewan where high freeze–thaw rates were deemed responsible. These microbands were attributed to horizontal ice lens formation, succeeded by a thawing phase when the 'finer particles exist as a fluid suspension through which coarser materials have time to settle, resulting in the physical separation of particles within the bands' (Mermut & St. Arnaud 1981, p. 586). This mechanism differs from others proposed before or subsequently, in that it invokes a downward movement of the coarser rather than finer particles to produce the relative concentration of the latter on aggregate surfaces.

Romans *et al.* (1966, 1980) and Romans & Robertson (1974) suggested that the silt droplet fabrics, recognized in the mountain soils of Britain and having similar characteristics to these banded and microbanded fabrics, result from the release of silt-rich water by the final melting at the base of a frozen soil crust into a desiccated horizon above permafrost. Associated silt cappings (Romans *et al.* 1980), similar to the rare silty clay, discontinuous cappings on vertically oriented, prolate coarse sand and gravel clasts in the upper 30 cm of the soil at Ipswich Airport, may also be formed by this process. In contrast to Romans *et al.* (1966), who proposed a removal of meltwater from the upper part of the frozen layer by lateral drainage and drying winds before final meltout of the basal ground ice zones, Harris & Ellis (1980) suggested that a perched water table develops above the frozen subsoil and, after ground ice removal, there is rapid vertical drainage throughout the soil leading to capping of the coarse detrital grains.

Further alternative hypotheses have invoked the formation and melting of segregated ice as a major contributory factor to the genesis of both cappings and banded-type fabrics. FitzPatrick (1971) suggested that these cappings develop by the infilling of pores resulting from the melting of ice sheaths above grains.

The duplex textural lamellae features in the soil at Ipswich Airport most closely resemble the sorted lamellae structures described from Quaternary soils in France or Belgium, and from cryogenic soils in northern latitudes by Van Vliet-Lanoe (1976, 1982). These consist of a lamella of fine material (with a striated b-fabric) that overlies groundmass, and is itself overlain by a zone of loose uncoated coarser grains. The major difference between these and the duplex textural lamellae features is the presence of a marked vertical graded bedding of the upper coarse lamella (indicative of sorting processes), the absence of which at Ipswich Airport probably reflects the dearth of suitable mixed grain sizes.

In accordance with some of the conclusions of Van Vliet-Lanoe (1976, 1982), it is suggested that the duplex textural lamellae features originated by freeze–thaw processes associated with segregation of ice. On slow winter freezing, ice segregation occurred within horizontal zones, which resulted in the desiccation, fracture and fragmenting of coatings around grains immediately above and below. Within the ice-segregated zone, the clay coatings may also have fractured after freezing and expansion of interplatelet water. Freezing of capillary and adsorbed water had a stabilizing influence on the coatings as the cation concentration consequently increased. However, the sudden dilution brought about by the melting of the ice during the spring thaw led to dispersion of some clay-size particles (Van Vliet-Lanoe 1982) from the coatings and translocation with any loosened fragmented coatings. Deposition of the suspension occurred at the sub-horizontal base of the segregated ice cast, where the lower lamella was initiated, leaving the upper contrasted lamella relatively deficient in clay. The unistrial b-fabric of this lamella reflects a preferred orientation of the clay platelets parallel to the horizontal axis of the feature, and is probably due to a combination of sedimentation/drying and stress imparted normal to their long axes by later generations of segregated ice. During subsequent freezing, a vertical sorting process, involving the downward migration of fine materials (fragmented coatings and clay-size particles) in the manner proposed by Corte (1961), may have augmented the general processes leading to the formation of the duplex textural lamellae features. Successive cycles of freezing and thawing were probably necessary for their full development, a conclusion substantiated by the experimental work on banded fabrics reported by Dumanski (1964).

(*d*) *Silt translocation*

The enclosure of some sand grains coated with impure clay within localized concentrations of silt grains in the uppermost horizons of the buried soil represents a phase of silt translocation and void infilling that must postdate the formation of the clay coatings. Similar 'embedded grain argillans' have been attributed to the incorporation of coated grains into a sediment during transport and were not therefore considered *in situ* (Bullock & Murphy 1979). Such a hypothesis is not applicable to this soil as there are rare *in situ* fractured bridge coatings and an *in situ* shattered, coated clast associated with these embedded grain coatings in the same thin section. Physical translocation of silt-size particles in soils is an established process (Federoff 1974), which is more commonly thought to occur in cold, moist environments (Federoff & Goldberg 1982), particularly those characterized by seasonal freezing and thawing régimes (Romans *et al.* 1980). The unimodal size distribution of these silt coatings and infillings, and consequent absence of clay must reflect either a deficiency at source in the eluvial horizon, or an efficient flushing through the profile (Federoff & Goldberg 1982). Alternatively, there may have been some vertical sorting akin to that proposed for the second illuvial phase, so that some of the lower impure/speckled clay coatings are contemporaneous with the silt infillings. The silt grains are predominantly quartz or other minerals, although some fragmented clay coatings are rarely incorporated within the coarse infillings. Periodic rapid flow rates, possibly after ice melt, may also have led to the translocation and rounding of fragmented clay coatings that now occur as clusters in the larger packing voids lower down the profile.

(*e*) *Thermal contraction and wedge formation*

Larger-scale evidence of the influence of cryogenic processes on the development of the soil is demonstrated by the two wedges and number of infilled fissures. Although some wedges are attributed to desiccation or solution (Black 1976), it is suggested that these were initiated by thermal contraction at sub-freezing temperatures. Both display the classical upturning of adjacent horizons that is often associated with ice-wedge development (Black 1976). However, as ice wedges are by definition permafrost phenomena (Mackay & Matthews 1983), it is preferable to assign a less genetic term such as 'soil wedge' to these features as they are of much smaller dimensions than reported casts of ice wedges developed in permafrost, and may just

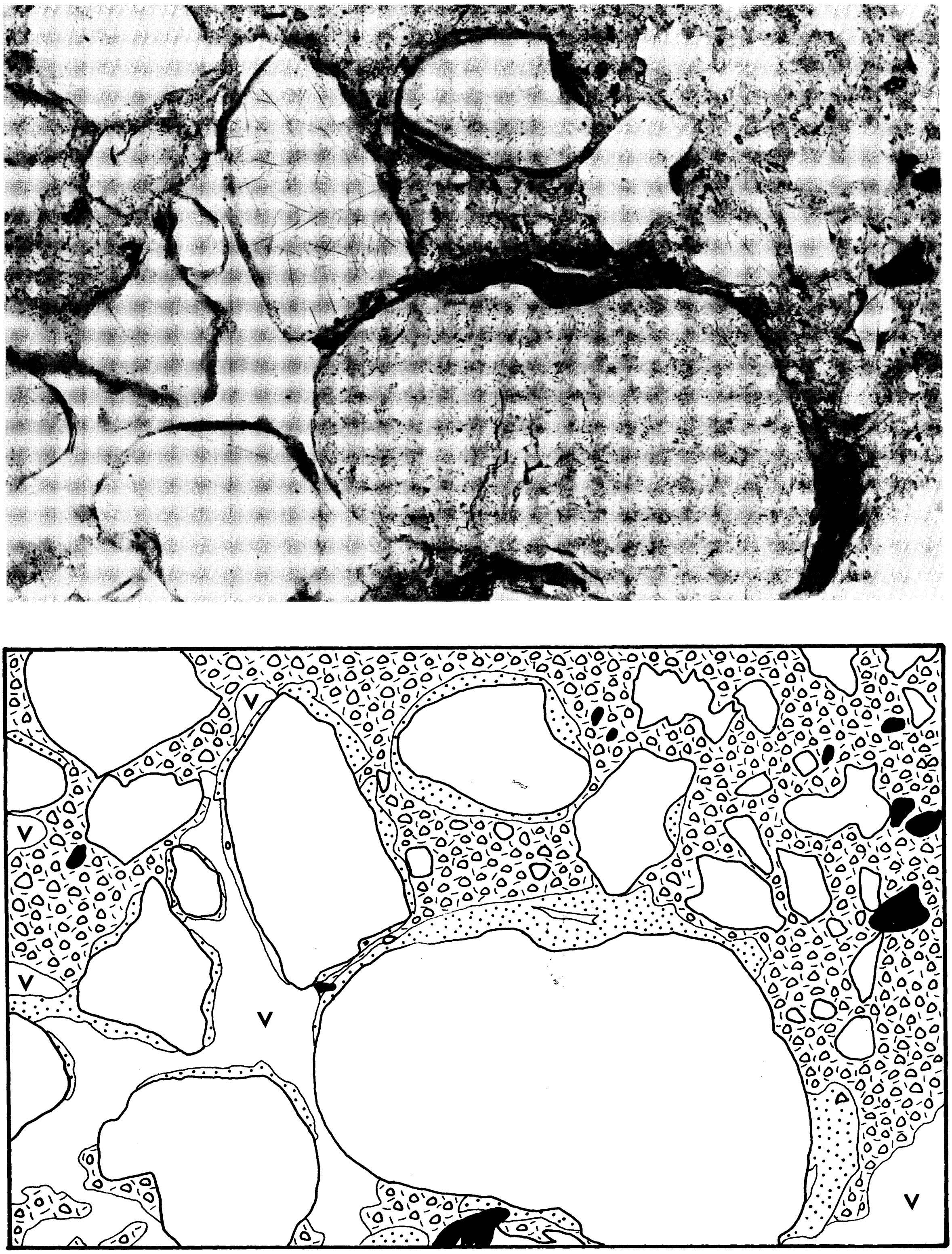

FIGURE 4. Photomicrograph (top) and interpretative diagram (bottom) of sand grains, coated with impure clay and embedded within groundmass in thin section 1b. Plane polarized light (PPL); horizontal frame length (HFL) = 1.3 mm.

KEY

	Mineral grains or nodules	L	Limpid clay
V	Void		Speckled clay
	Coatings around grains		Speckled/impure clay
	Fractured coatings		Silty clay groundmass
	Fragmented coatings		Sesquioxidic (pure or strongly impregnated)

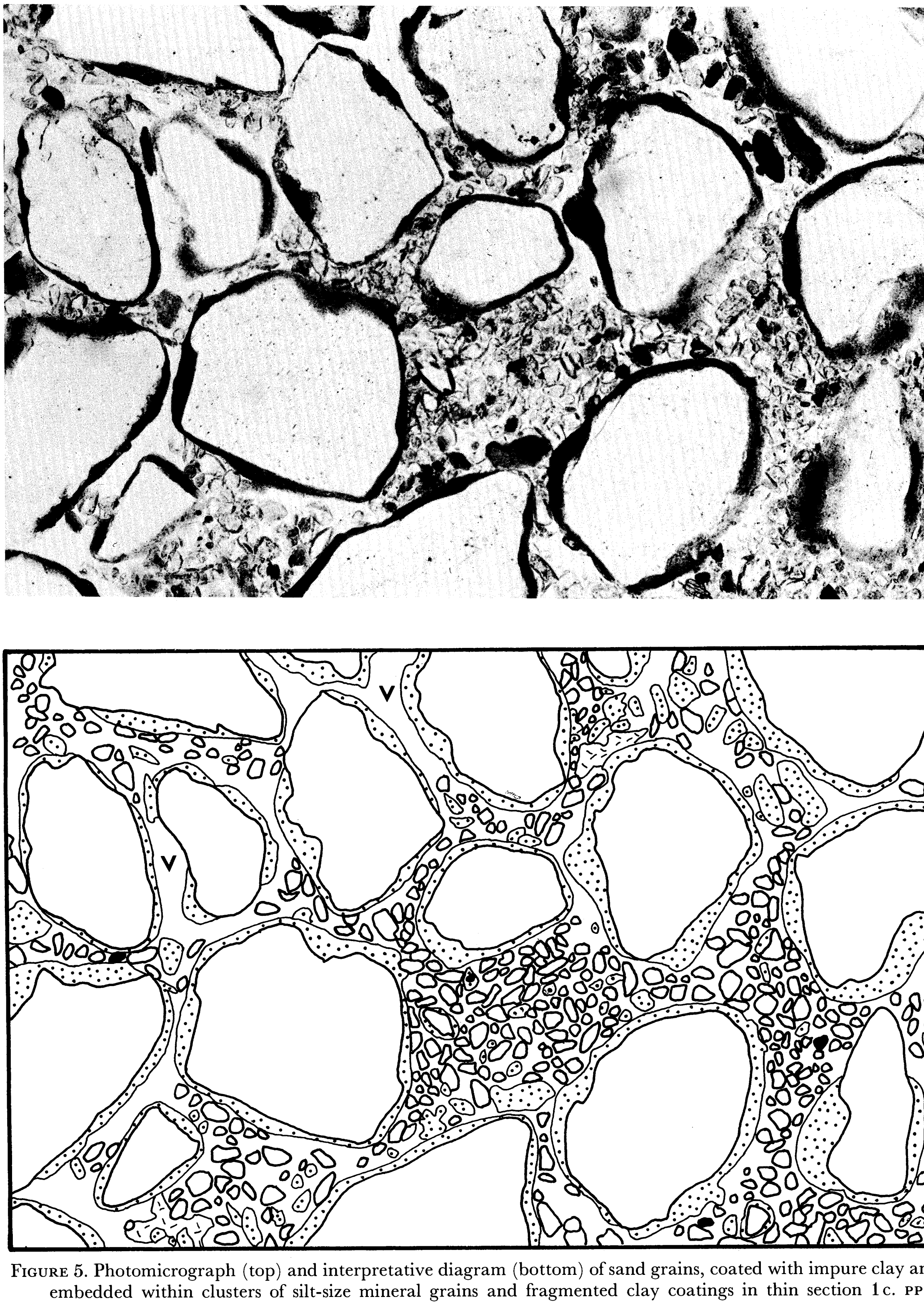

FIGURE 5. Photomicrograph (top) and interpretative diagram (bottom) of sand grains, coated with impure clay and embedded within clusters of silt-size mineral grains and fragmented clay coatings in thin section 1c. PPL; HFL = 1.3 mm (key as for figure 4*b*).

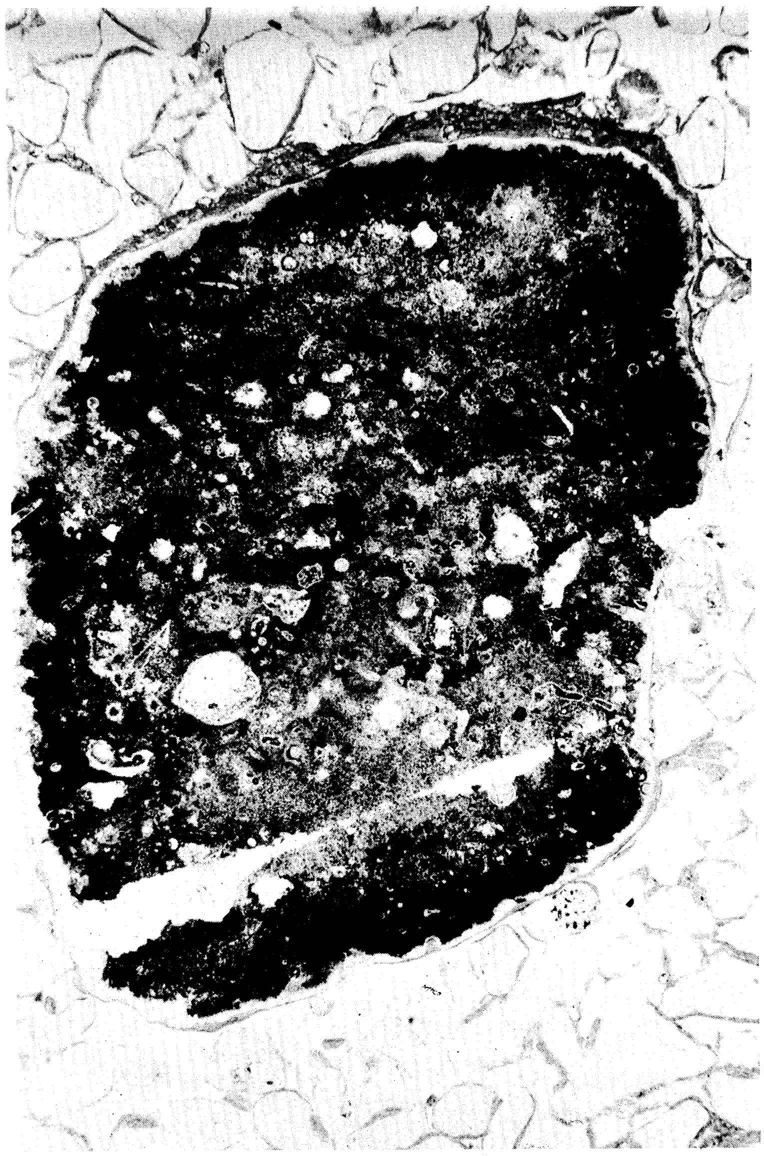

FIGURE 6. Photomicrograph of a silty clay capping upon a chert clast in thin section 1c. PPL; horizontal frame width (HFW) = 3.4 mm.

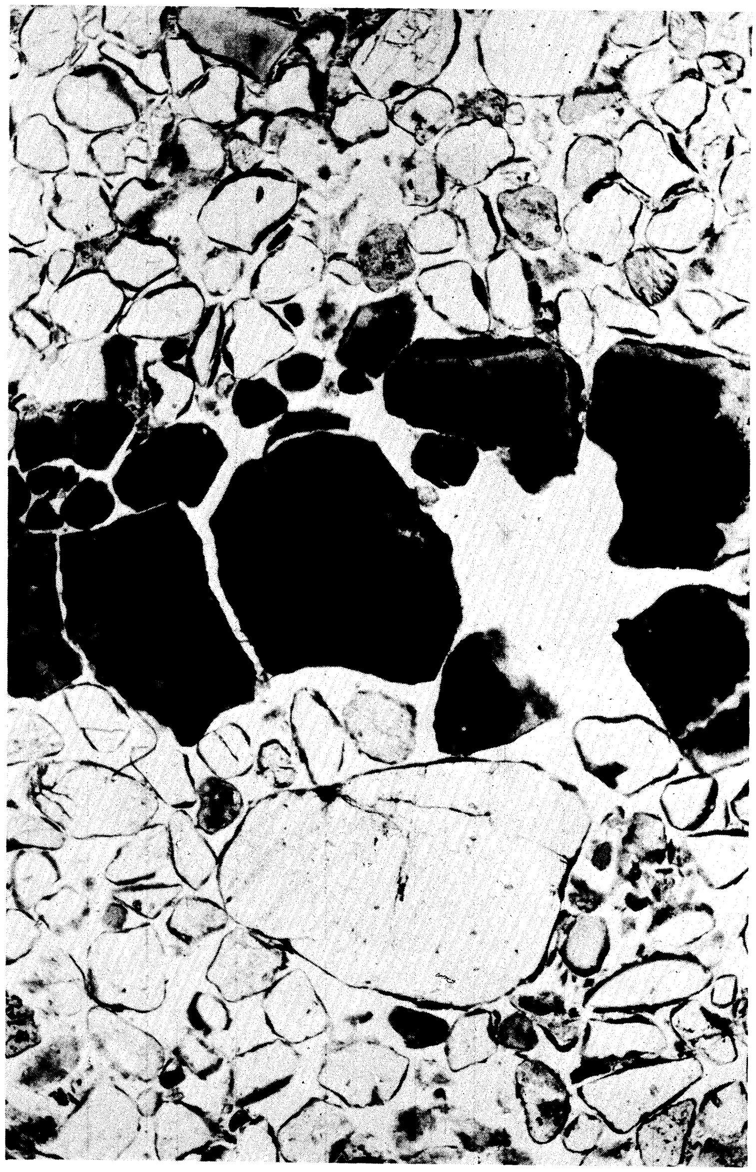

FIGURE 7. Photomicrograph of a chert clast fractured into conjoinable fragments in thin section 1c. PPL; HFW = 3.4 mm.

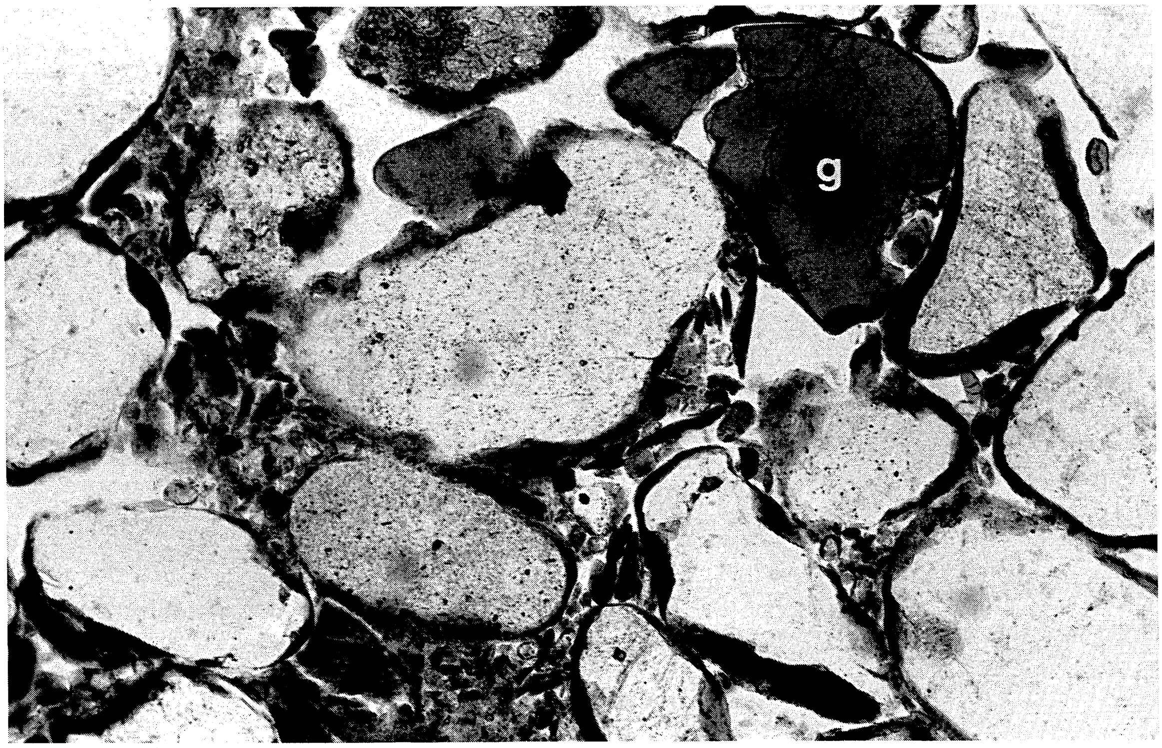

FIGURE 8. Photomicrograph showing a weathered (fragmented) glauconite grain (g) in thin section 2d. PPL; HFL = 1.3 mm.

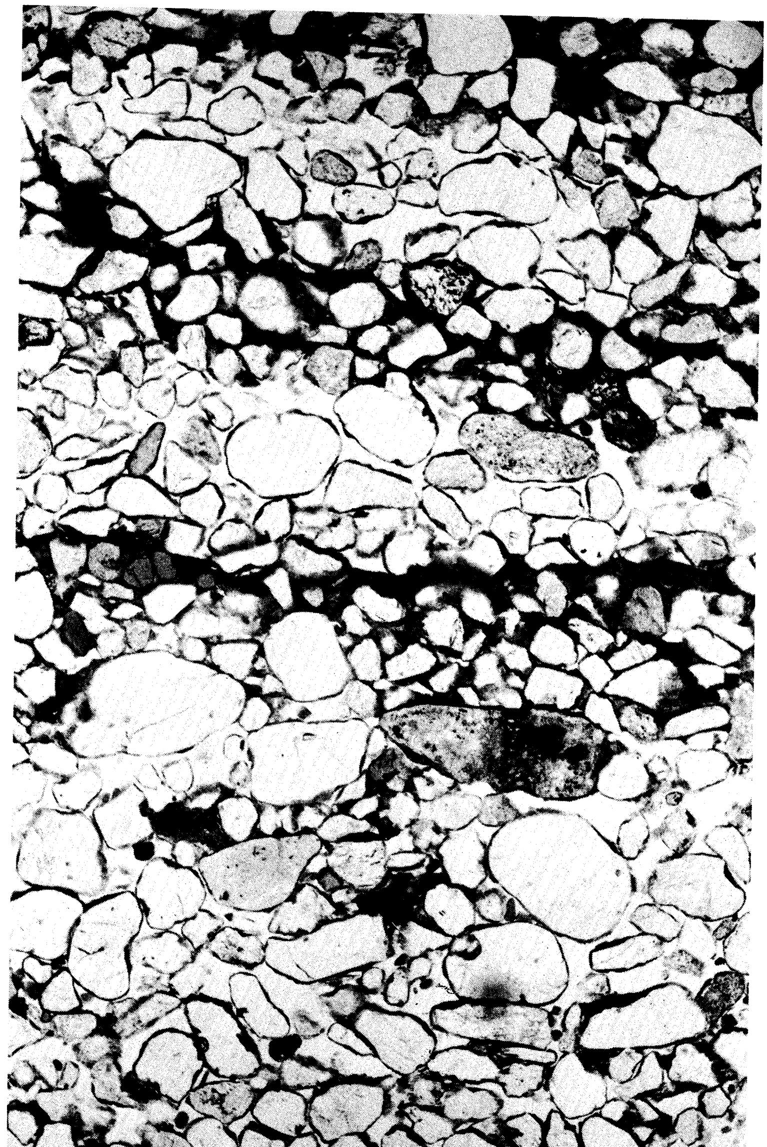

FIGURE 9. Photomicrograph of duplex textural lamellae a-features in thin section 2e. PPL; HFW = 3.4 mm.

FIGURE 10. Contact print of impregnated block adjacent to surface used for thin section 2e, which shows platy structure (black areas are voids). HFW = 5 cm.

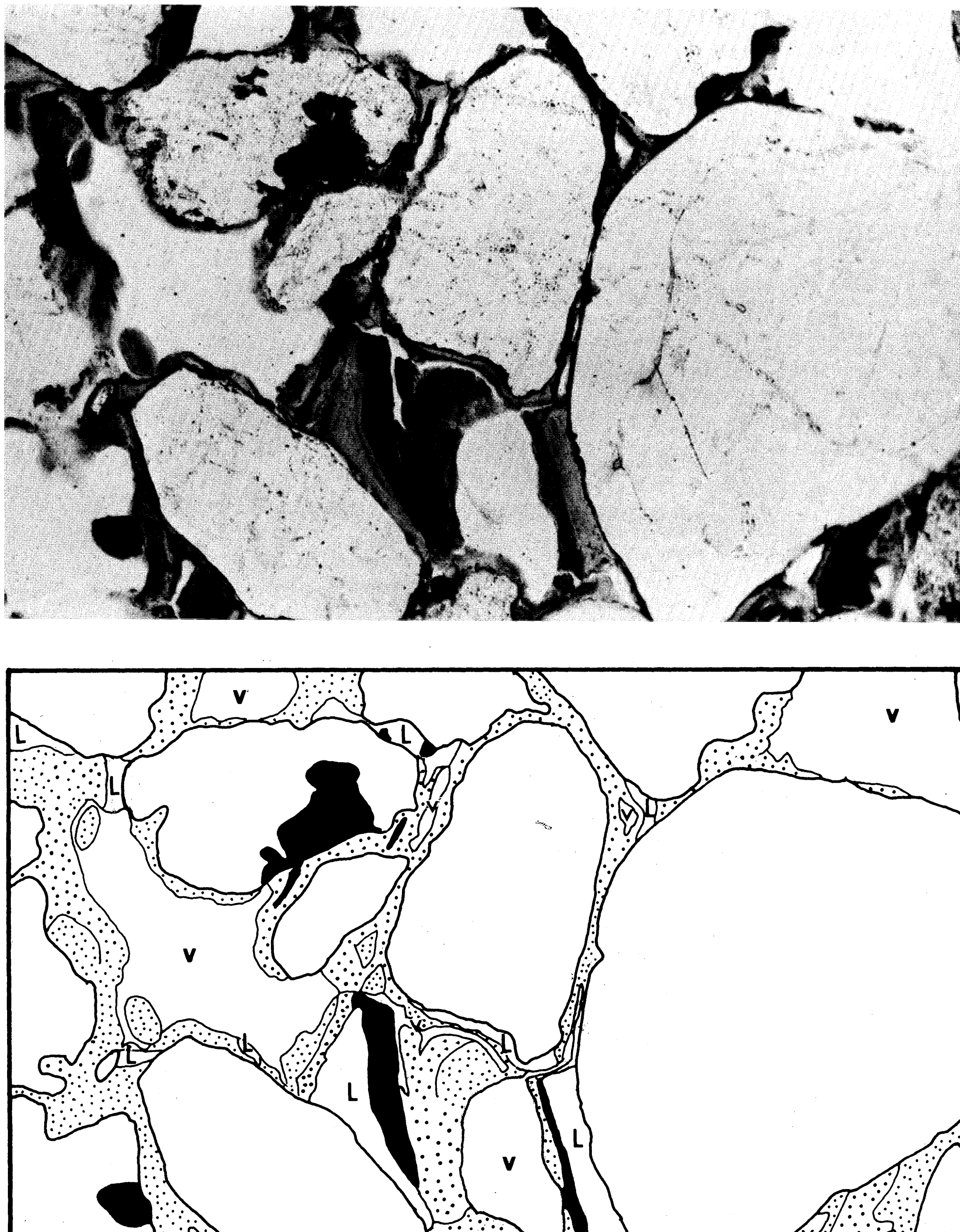

FIGURE 11. Photomicrograph (top) and interpretative diagram (bottom) of limpid clay coatings around sand grains which are postdated by complex speckled–impure clay coatings in thin section 1e. PPL; HFL = 1.3 mm (key as for figure 4*b*).

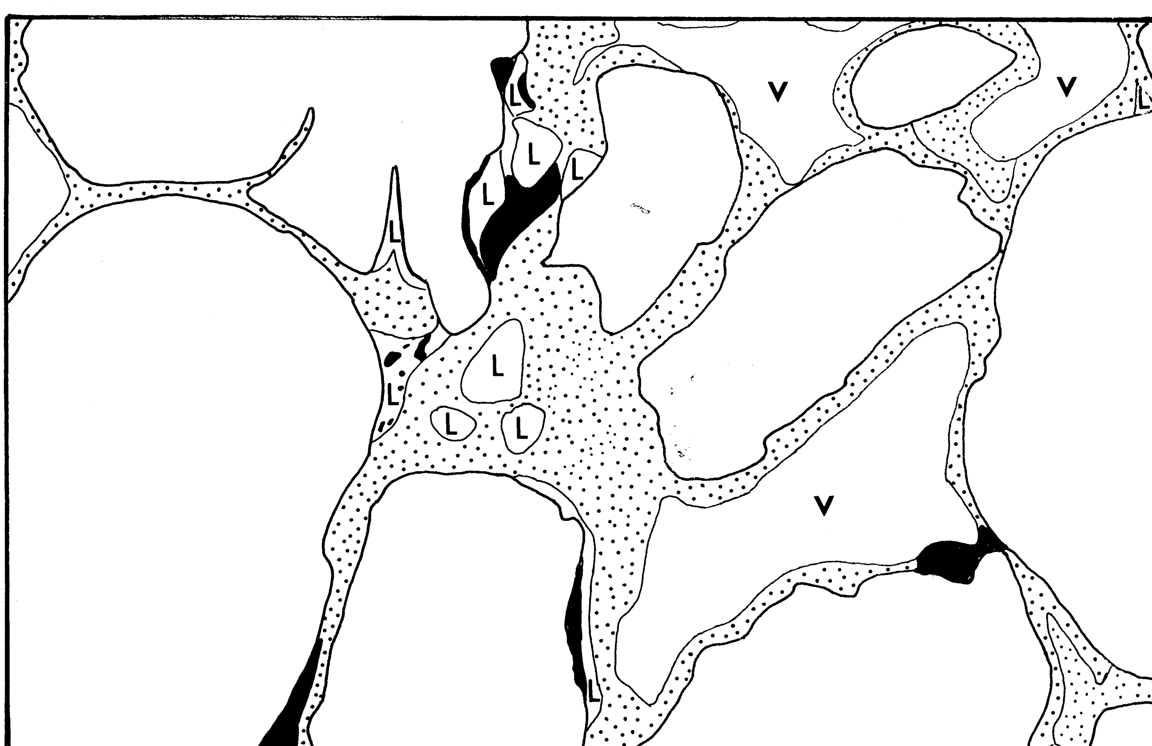

FIGURE 12. Photomicrograph (top) and interpretive diagram (bottom) of limpid clay coatings around sand grains with adjacent fragmented coatings of similar composition embedded within speckled–impure clay coatings in thin section 1e. PPL; HFL = 1.3 mm (key as for figure 4*b*).

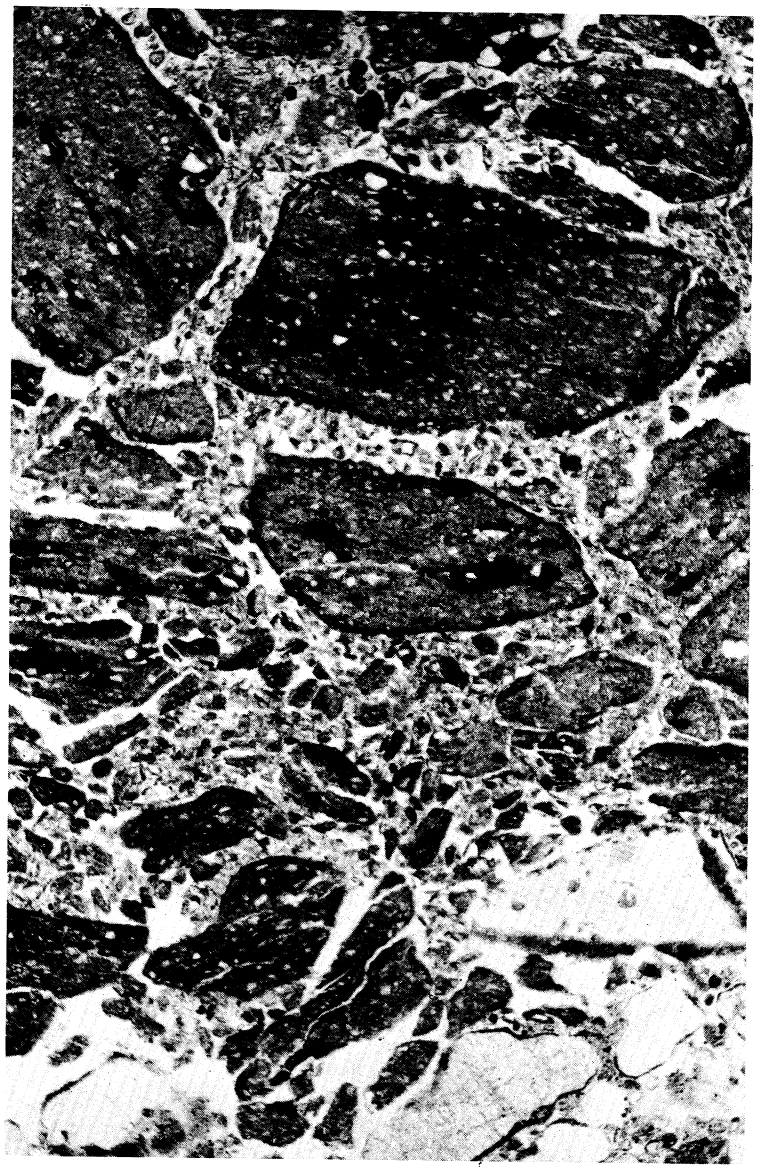

FIGURE 13. Photomicrograph of fragmented micaceous, silty clay lenses in thin section 2d. PPL; HFW = 3.4 mm.

indicate seasonally frozen ground (French 1976). Seasonal soil wedges have not often been described in the literature (Black 1976) as they would normally be short-lived and destroyed by summer melt, movement and collapse processes. However, preservation of seasonal wedge casts in the soil at Ipswich Airport is possible because there is no evidence for anything other than small-scale freeze–thaw disruption features. Thus a development sequence responsible for the formation of the complex soil wedge in profile 1 can be envisaged in terms of cycles of winter thermal contraction and desiccation, and spring and summer melting. The contraction led to production of a frost crack that was infilled by slumping of material, initially from the top of the Bt horizons, but later from the overlying pale brown horizon. The irregular shape of the basal part of the wedge, and the feeder vein cast extending to the top of horizon 6, confirm the cyclic nature of the process with later contraction cracks departing from the path of earlier infillings. The occurrence of both uncoated and coated grains in the infill may indicate a locally derived aeolian component, although the bare grains could have moved from a sandy part of the eluvial horizon before its removal, or have had their coatings removed by fracture and fragmentation.

The upturning of the adjacent horizons on the left-hand side of the soil wedge in profile 1 was probably caused by the expansion of warming ice, which may have originally accumulated in the contraction crack at times during the winter in the form of hoar frost (FitzPatrick 1974) or (temporary) refreezing of meltwater percolating from the thawing upper layers. This may have been enhanced by years when complete thawing did not occur during the summer, and effective permafrost conditions were temporarily produced. Evidence of similar deformation structures on the right-hand side of the wedge is absent as the low-angle slope of the boundary between the soil and S2 suggests that part of the soil has slumped into the wedge. Ice expansion may also provide the explanation for the upturned horizons to the right of the simple soil wedge in profile 2, particularly as the extension of the infill above the buried soil surface and into the S2 could be due to a similar process (Black 1976).

A deterioration of climate with time is the basis for the development sequence formulated above for the buried soil at Ipswich Airport. The existence of such a sequence is further demonstrated by the common greyish brown, sandy clay fissure-shaped zones extending vertically from the truncated surface of the soil. The thin section taken through one of these features demonstrates that they are second-phase illuvial clay infillings of fissures that probably date from the earliest stages of thermal contraction. As such, they represent a transitional stage between the phase of coarse clay translocation with some related coating disruption, and the phase of intense thermal contraction and associated slump infilling.

(*f*) *Gleying, weathering and eluvial horizon formation*

Ferruginous hypocoatings and segregations within the lens aggregates testify to the importance of iron mobilization processes during the development of the soil. Segregations and superimposed accretionary halo nodules (glaebular halos: Brewer (1976)) across coatings higher up in the profiles suggest that redistribution of iron took place primarily after accumulation of significant quantities of illuvial clay, but before the major phase of disruption. Segregation and migration of iron oxides have been experimentally shown to occur during the early stages of the freezing process (Bertouille 1972), and this may account for some of these features. Alternatively, redistribution of iron may have resulted from surface-water gleying, a process resulting from the existence of impermeable lenses or the build up of high illuvial clay contents, leading to periodic accumulation of water. High $Fe_o : Fe_d$ values, as obtained from the less than 2 mm fractions of selected horizons, are frequently associated with horizons that have undergone surface-water gleying and redistribution of crystalline iron oxides in more amorphous forms (Moore 1973). However, the substantially lower values of the more mobile clay-size fractions suggest that recrystallization has occurred after redistribution, and that the Fe_o values of the less than 2 mm fractions reflect appreciable sand-size magnetite contents (Rhoton *et al.* 1981), a conclusion substantiated by the opaque heavy-mineral composition of the sand.

The normal colour microlaminations within particular coatings clearly indicate that the clay and iron were initially translocated in close association with each other. However, the rare isotropic (pure ferruginous?) microlaminations may demonstrate periodic departures from this rule.

The clay-size fractions of the reddish horizons (1/9 and 2/9) in the soil both contain very large amounts of goethite. Haematite is also present, a mineral that has been shown to be responsible for reddish colours in soils even when present in small amounts (Kemp 1985*c*).

The appreciable quantities of iron oxides and clay accumulated in these buried illuvial horizons must be derived from overlying eluvial horizons that have been subsequently removed. It is difficult to conceive the origin of such components if the eluvial horizon was developed in the same sands and gravels that compose most of the parent material of the illuvial horizons. Primary sources of both components would have been absent, whereas neoformation is hardly tenable because of the dearth of evidence for *in situ* weathering of the predominantly residual mineral assemblages. Even the *in situ* alteration of glauconite grains is insignificant in this context.

The eluvial horizon must have developed in a material containing abundant supplies of easily-weatherable minerals or sufficient quantities of iron oxides and clay or both. The most logical explanation, therefore, is to interpret S2 in terms of a transported eluvial horizon. Its sand and clay fractions are mineralogically similar (at least in types of species present) to lower horizons in the soil. Its large silt and small clay and Fe_d contents would account for the source of both minor quantities of translocated silt at the top of the illuvial horizons, and the accumulated clay and iron oxides throughout both profiles. Presumably the layer was originally deposited as overbank sediments in a low-energy depositional environment similar to that responsible for the fine-textured lenses at the base of profile 1. Heavy and light separates from sand and silt fractions of both these lenses and the reworked eluvial horizon contain quantities of phyllosilicates that may have provided an additional neoformed source for the iron oxide and clay accumulations.

The sand grains, coated with impure clay and embedded within the groundmass provide some substantiation for the solifluction origin of S2. These features indicate truncation and movement of not only the eluvial, but also the upper part of the illuvial horizons of the soil.

Clay mineral alterations, preceding clay translocation, may also be inferred from the contrasting mica and interstratified smectite proportions of the clay-size fractions from the top and bottom of the soil. The transformation of micas to expanding minerals, accompanied by release of potassium and possibly iron, is an established soil process commonly occurring in temperate environments. The discrete vermiculite component, recognized within the interstratified smectite in the eluvial and uppermost illuvial horizons, is unlikely to reflect *in situ* weathering bearing in mind the translocated nature of the clay in the latter. A more logical explanation is that it is present as a component only in the coarser clay, a size fraction more dominant in these horizons.

(*g*) *BSG and S1 units*

The BSG can be distinguished from the WSG on mineralogical criteria. Apart from having larger amounts of heavy minerals (particularly opaque grains) in the fine-sand fractions, this upper glacifluvial unit has small, yet significant quantities of easily weatherable minerals (collophane and apatite) to complement its stable garnet- and tourmaline-dominated heavy mineral assemblages. The WSG, however, have more restricted zircon- and tourmaline-dominated assemblages with no weatherable minerals. These differences suggest that although both sedimentary units were derived from a strongly weathered source, the Barham Formation was enriched by fresh minerals associated with a glacial event (Rose *et al.* 1976).

The similarity in heavy mineralogy of S1 to that of the BSG and difference from that of the underlying S2 suggest derivation from the Anglian ice sheet. In the absence of a detailed analysis of this horizon, it is tentatively related to a later solifluction event, before deposition of the glacifluvial BSG. The concurrent micro-involutions at the junction of these two deposits and at the boundary between the lower one and the soil surface are similar to structures attributed to cryoturbation (Gladfelter 1972). Their absence along other parts of the section, however, may imply a more local significance, possibly related to disruption and shearing during deposition of the upper solifluction unit.

8. Summary and conclusions

A development sequence can be reconstructed for the buried soil at Ipswich Airport on the basis of the feature and property associations discussed in the previous section (figure 14). This sequence began with deposition of the sand and gravel (WSG) parent material within a proto-Thames floodplain. During sedimentation, there were periodic quiescent phases when finer textured lenses were deposited. Similar overbank material was probably the final layer to be deposited before commencement of soil formation. After establishment of a land surface, fine clay was translocated from the overbank sediments down into the lower sands and gravels.

Weathering processes probably began during this first illuvial phase and continued throughout the remainder of the development cycle. Similarly, iron began to be mobilized and recrystallized at this stage and further segregation occurred during later phases of surface-water gleying.

Localized disruption of some limpid coatings by biotic, shrink–swell or frost processes occurred before or during the transition of a second illuvial phase, which was characterized by translocation of coarse and fine clay as well as fine silt. It is suggested that this change in composition of illuvial material corresponded to a deterioration in climatic conditions, perhaps from the optimum of a temperate stage to a later cooler part of the same stage. Vertical sorting of the illuvial clay led to an upward growth in the Bt horizons, as the less mobile coarser clay was deposited higher up the profile than the finer material. Towards the end of this second illuvial phase, the environment had deteriorated to one characterized by seasonally frozen ground. Small-scale contraction cracks developed, coatings were fractured and fragmented and characteristic cryogenic features such as silty clay cappings and duplex textural lamellae

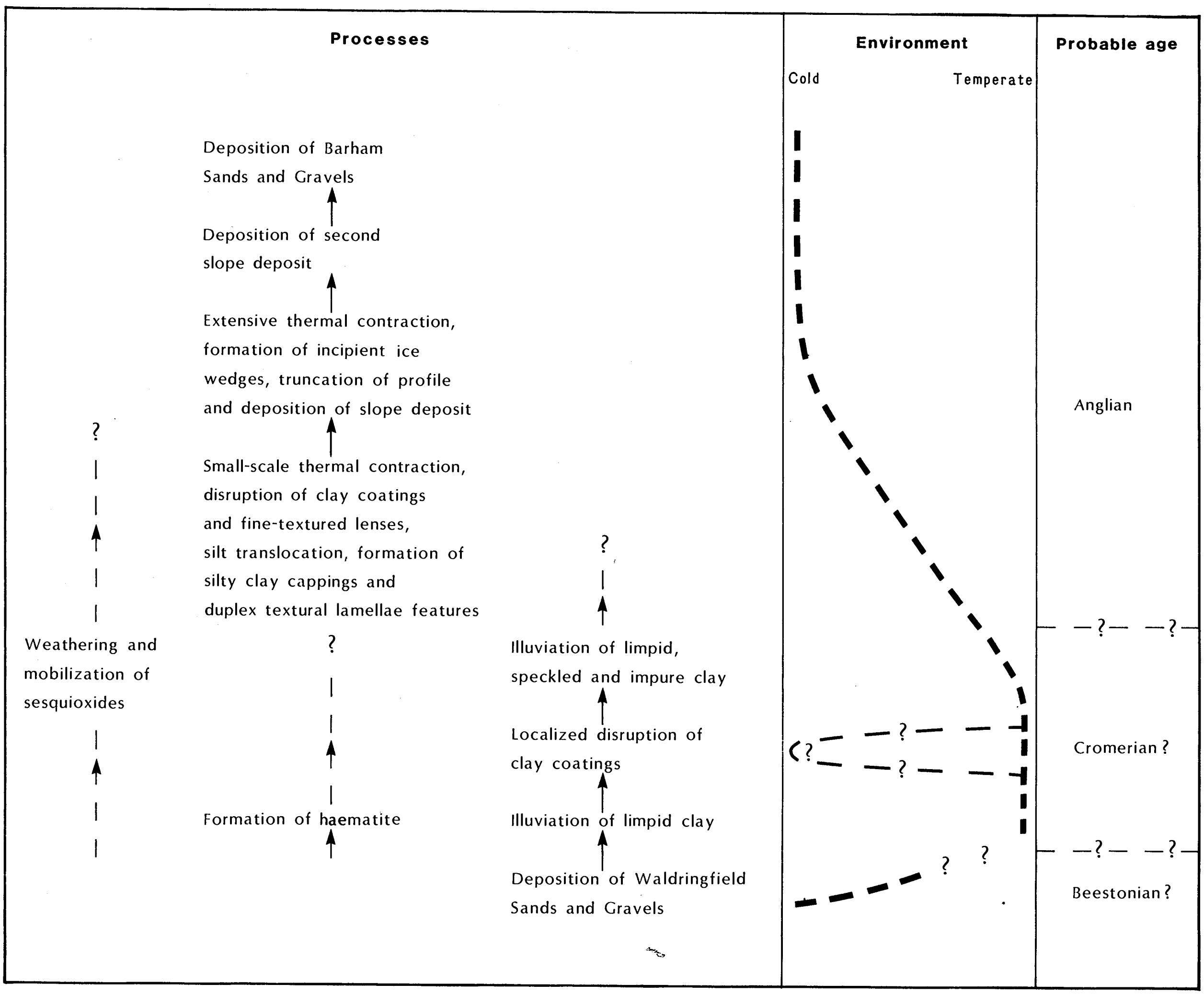

FIGURE 14. Proposed development sequence for the buried soil at Ipswich Airport.

features formed. Disruption was only localized, however, and not sufficient to cause extensive large-scale deformation of the soil, as is often the situation with seasonally-active freeze–thaw processes. Low moisture contents at the time of freezing may account for this, although sufficient water must have been available at times after thawing for the translocation of silt into the upper parts of the illuvial horizons.

Further deterioration of climate led to formation of larger-scale contraction cracks and soil wedges. Incipient ice wedges may also have developed under temporary permafrost conditions. Infilling of these wedges was closely associated with erosion and mixing of the eluvial horizons, processes that led to the soil profiles becoming truncated and covered by material derived largely from the eluvial horizons of adjacent areas. A second solifluction deposit predated complete burial of the soil by the glacifluvial outwash sands and gravels of the Anglian ice sheet.

Previous studies in Britain have tended to interpret buried soils or relict features from non-buried soils in terms of series of discrete time intervals. Stable phases of soil formation are ascribed to temperate stages and unstable phases of erosion or disruption to cold stages (Bullock

& Murphy 1979). This study, however, has provided evidence for a more realistic transition between these two extremes with pedogenic processes changing more gradually in phase with the environment.

According to the regional stratigraphy outlined by Rose *et al.* (1976), the soil at Ipswich Airport is a composite of the Valley Farm and Barham Soils. Assuming the Beestonian and Anglian ages of the Waldringfield and Barham Sands and Gravels (Allen 1983) are correct, the soil at Ipswich Airport could have developed during the Cromerian and early parts of the Anglian Stages. Such a chronology would not be in dispute with the soil/environment development sequence at the site, which proposes a simple deterioration from a climatic optimum until the time of burial (figure 14). However, much depends on the status of the first disruption phase. If the fragmentation of the limpid coatings does represent a sharp climatic oscillation, the stratigraphic implications may be more complex than portrayed.

The author extends his sincere thanks to Mr J. Rose, Dr P. Bullock and Dr J. A. Catt for their advice and helpful criticism throughout the course of this work and on earlier drafts of this paper. Receipt of a N.E.R.C. Studentship held jointly at Birkbeck College, London University and Rothamsted Experimental Station, Harpenden, U.K., is also gratefully acknowledged.

Additionally, the author thanks Dr P. Allen for discovering the site and kindly allowing him to work on it, Mr G. Brown and Dr I. Wood for providing the data on iron oxides, Mr C. P. Murphy, Mr R. M. Bateman and Dr P. Loveland for advice on aspects of micromorphology, optical and X-ray diffraction mineralogy respectively, and finally Mr I. Fullerstone for making many of the thin sections.

Appendix 1. Description of profile 1

horizon	
1 20–75 cm†	Yellowish brown (10YR 5/6); slightly stony medium sand; mainly small subrounded stones; single grain; abrupt wavy boundary to:
2_u 75–90/98	yellow (10YR 7/8); very slightly stony medium sand; mainly very small rounded stones; single grain; abrupt irregular boundary to:
2_l 75–108	brownish yellow (10YR 6/6); very stony coarse sand; mainly small and very small rounded stones; single grain; sharp irregular boundary to:
4 108–116/130	pale brown (10YR 6/3) with a 1 cm thick strong brown (7.5YR 5/8) horizontal band at 100 cm; moderately stony loamy sand; mainly very small and small rounded stones; single grain; sharp irregular, variable boundary to 6 and clear wavy boundary to:
5 130–136/150	brownish yellow (10YR 6/8) merging to yellow (10YR 7/8) at base; very slightly stony medium sand; all small subrounded stones; single grain; sharp irregular boundary to:
6 116–125/128	brownish yellow (10YR 6/6) with several dark greyish brown (10YR 4/2) vertical fissure-shaped zones (up to 1 cm thick); very slightly stony sandy loam; mainly very small rounded stones; massive; sharp smooth boundary to:
7	reddish yellow (7.5YR 6/8) with common very fine distinct yellowish

† Depths refer to distance beneath highest point of the excavated surface (cf. figure 3).

125/128–150 brown (10YR 5/4) mottles and several interconnected dark greyish brown (10YR 4/2) sub-vertical fissure-shaped zones (sandy clay and up to 1.5 cm thick); very slightly stony sandy loam; mainly small subrounded stones; marked upturning of horizon on the left side of 5 adjacent to the sub-vertical/sub-horizontal boundary change with 4. On the opposite side there are no deformation structures and the boundary slopes at a consistent 45° angle; massive; sharp wavy boundary to:

8 150–152/155	brown (10YR 5/3); very slightly stony loamy sand; mainly very small rounded stones; sharp clear boundary to:
9 152/155– 189/193	reddish yellow (7.5YR 6/8) with a strong brown (7.5YR 5/8) sharply bounded sub-horizontal band (4 cm thick) at 168 cm; slightly stony sandy loam; mainly small subrounded stones; massive to single grain; common prominent clay coatings all around stones; gradual irregular boundary to:
10 189/193–215	strong brown (7.5YR 4/6); moderately stony loamy sand; mainly small subrounded stones; single grain; common faint clay coatings mainly restricted to upper surfaces of stones; clear wavy boundary to:
11 215–252	strong brown (7.5YR 4/6); moderately stony loamy sand; mainly medium subangular stones; single grain; clear wavy boundary to:
12 252–271	brown (7.5YR 5/4); very slightly stony medium sand; mainly medium subangular stones; single grain; few sub-horizontal sandy loam lenses (1 × 0.5 cm); sharp broken boundary to:
13 271–	light yellowish brown (2.5Y 6/4) with common fine prominent strong brown (7.5YR 5/8) mottles; sandy loam with common clearly bounded sub-horizontal sand lenses (2–10 × 1–3 cm) associated with mottles; massive to single grain.

Appendix 2. Description of profile 2

horizon	
1 0–50/70 cm†	Yellowish brown (10YR 5/4); slightly stony medium sand; mainly small subrounded stones; single grain; sharp wavy boundary to:
2 50–70	yellow (10YR 7/8); medium sand; single grain; abrupt wavy boundary to:
3 70–105	yellowish brown (10YR 5/8); very slightly stony sandy loam; mainly medium subrounded stones; massive; sharp irregular boundary to:
4 70–97/110	pale brown (10YR 6/3); moderately stony loamy sand; mainly medium and small subangular to angular stones; single grain; sharp irregular boundary to 6 and to:
5 97–132	light yellowish brown (2.5Y 6/4); very slightly stony coarse sand; mainly small rounded stones; single grain; sharp vertical boundary to 7 and sharp irregular boundary to:
6	yellowish brown (10YR 5/4); very slightly stony loamy sand; mainly very small

† Depths refer to distance beneath highest point of the excavated surface (cf. figure 3).

100/110–107–114	rounded stones; single grain; marked upturning of horizon on the right side of the boundary with 5; abrupt wavy boundary to:
7 107/114–140	brown (10YR 5/3) with common extremely fine distinct brownish yellow (10YR 6/6) mottles and several interconnected dark greyish brown (10YR 4/2) sub-vertical fissure-shaped zones (up to 1 cm thick) extending from the top of 6 into 8; very slightly stony sandy loam; mainly small and very small rounded stones; single grain to massive; abrupt wavy boundary to:
8 140–145	strong brown (7.5YR 4/6) with common extremely fine distinct yellowish brown (10YR 5/6) mottles; slightly stony sandy loam; mainly medium subangular stones; massive; abrupt wavy boundary to:
9 145–154	reddish brown (5YR 4/4); very slightly stony loamy sand; mainly medium subangular stones; massive; clear wavy boundary to:
10 154–207/210	strong brown (7.5YR 5/6); moderately stony loamy sand; mainly very small rounded with a few medium subangular stones; single grain; few distinct clay coats all around stones; gradual wavy boundary to:
11 207/210–235	strong brown (7.5YR 5/8); moderately stony loamy sand to medium sand; mainly very small and medium subrounded stones; single grain; diffuse wavy boundary to:
12 235–	brown (7.5YR 5/4); very slightly stony coarse sand; mainly small and medium subrounded stones; single grain.

Appendix 3. Glossary of micromorphological terms

(a) *General outline*

The terminology is largely based upon that provided by Bullock *et al.* (1985), although certain terms may have slightly different connotations as only a draft version of the system was available at the time of study. Obvious or well-established terms, particularly those used by Brewer (1976), are not included in this glossary.

Pedofeatures are defined by Bullock *et al.* (1985) as 'discrete fabric units present in soil materials recognizable from adjacent material by a difference in concentration in one or more components'. The 'pedo-' prefix implies a definite pedogenic origin although similar features may result from both pedogenic and non-pedogenic (particularly geological) processes (Brewer 1972; Walker *et al.* 1978). The use of an additional term, geofeature, might obviate this difficulty, although it would introduce an unwarranted increase in the interpretative level required for what is basically a descriptive terminology. Alternatively, the pedofeature concept can be discarded completely and replaced by a less stringent term such as *concentration feature* (Kemp 1985*b*). This is defined as a discrete fabric unit distinguishable from adjacent material by an increase in concentration in one or more components. The term is restricted to units having at least a potential pedogenic origin; obvious sedimentary banding associated with variable sorting or graded bedding is not included.

Groundmass is a general term for describing the fine material (micromass) and the coarse material. Coarse particles are those greater than 10 μm in minimum diameter and fine particles are less than 10 μm. Concentration features are considered separately and generally not included within either grouping, except where it is not possible to separate out such features adequately from the groundmass.

(*b*) *Groundmass*

The birefringence fabric (b-fabric) is approximately equivalent to the plasmic fabric (Brewer 1976) with five major divisions (undifferentiated, crystallitic, speckled, striated and strial). Only the following are appropriate to his paper.

1. Speckled b-fabric: small zones (a few micrometres) of orientation birefringence due to fine particle orientation.

(*a*) Stipple speckled: individual and isolated speckles.

(*b*) Mosaic speckled: birefringent streaks are in contact with each other resulting in a mosaic-like pattern.

2. Strial b-fabric: preferred orientation of large elongate birefringent streaks (often of several millimetres or centimetres in length), in which the particles show more or less simultaneous extinction under crossed polarized light.

(*c*) *Ferruginous concentration features*

Amorphous concentration features are concentration features that 'appear amorphous in plane polarized light and isotropic between crossed polarizers' (Bullock *et al.* 1985). Some of the material is likely to be partly or wholly crystalline, though its crystallinity is not recognizable under the magnification and light conditions used. Impregnative amorphous concentration features arise from the impregnation of groundmass or other concentration features; other features may be pure and isotropic, yet either translucent or opaque. The three major types of amorphous components are frequently differentiated on the basis of colour under oblique incident light (Kemp 1985*b*). The yellowish brown to orange- or reddish brown colours of the concentration features in thin sections from this study are attributed to the dominant presence of oxides and hydroxides of iron, though manganese may also be present in variable quantities. Consequently, they are referred to as ferruginous concentration features.

Three types of ferruginous concentration feature are important in this study:

1. segregations: impregnative concentration features which are frequently synonymous with ochreous mottles in the field;

2. hypocoatings: segregations adjacent to void or grain/aggregate surfaces;

3. nodules: impregnative or pure concentration features unrelated to voids, surfaces of grains and aggregates (Bullock *et al.* 1985). They have a regular circular shape and sharp boundary to the adjacent material (Bullock & Murphy 1979). Normal nodules have an undifferentiated internal fabric, while halo nodules have a crystalline or strongly impregnated core and a weaker impregnated cortex.

(*d*) *Textural concentration features*

Textural terms include limpid (fine clay), speckled (coarse and fine clay), impure (clay with included fine silt), silty clay, silt and other recognized particle size groupings.

There are five major terms that require definition as they are used in a different sense to Brewer (1976) and do not necessarily relate directly to Bullock *et al.* (1985).

1. Coatings: coats of specified material on void or grain/aggregate surfaces. These may

extend to form bridges between grains and eventually partly or completely infill the voids.

2. Compound coatings: a series of coatings of different texture or colour around the same void or grain/aggregate surface. A coating that 'postdates' or is 'inside' another coating is closer to the existing void. This refers to both grain and void compound coatings.

3. Cappings: coatings only on the upper surface of grains or aggregates.

4. Fractured coatings: coatings transversed by random fracture planes.

5. Fragmented coatings: equant to prolate features of variable angularity with internal laminations, texture and orientation similar to coatings. They may be loose or embedded within the groundmass or a coating (sharp boundary in plane polarized light). They are unrelated or adjacent to formative surfaces.

Two important characteristics of textural concentration features are their internal fabric and the degree of orientation of their components.

1. Internal fabric:

(*a*) non-laminated: concentration features are always non-laminated unless specified otherwise;

(*b*) microlaminated: alternating laminae (less than 30 μm) of different texture or coloured materials or both;

(*c*) laminated: alternating thick lamellae (greater than 30 μm) which are otherwise similar to (*b*).

2. Orientation:

(*a*) continuous: clay-size material exhibits extinction lines or extinguishes as a unit;

(*b*) flecked continuous: zones of continuous orientation;

(*c*) discontinuous: birefringent zones associated with non-birefringent zones.

Percentage cover of clay concentration features (% CCF) in thin sections is estimated by comparison to reference sections and expressed on a void- and gravel-free basis (Murphy & Kemp 1984).

A link capping is defined by Bullock *et al.* (1985) as a 'capping that covers the top surface of, and is supported by, two or more grains or aggregates'. They suggested that it has previously been described as banded fabric by Dumanski & St. Arnaud (1966). Either term is not satisfactory to describe one particular textural concentration feature identified in this study. It is a linear feature consisting of two lamellae. The lower lamella has few fine to medium silt mineral grains or fragmented coatings embedded within speckled or impure clay which has a unistrial b-pattern that is parallel to the lineation of the feature. This lamella has a prominent to distinct clear boundary to the adjoining groundmass or other concentration features below. Above is a lamella of uncoated or partly coated, loose sand grains which has a prominent sharp boundary to both the adjoining groundmass or concentration features and the lower lamella.

Van Vliet-Lanoe (1976) considered similar lamellae to comprise a sorted lamellae structure, although in her examples there was a marked downward vertical fining within the coarser components in the upper lamella. The clear contrast in particle size between the two lamellae warrants some textural emphasis in the naming of this concentration feature. Consequently, the term *duplex textural lamellae feature* is proposed and is used throughout. Less well-developed forms with no unistrial orientation or with poorly defined boundaries between individual lamellae are termed *duplex textural lamellae a-features*.

References

Allen, P. 1983 Middle Pleistocene stratigraphy and landform development of southeast Suffolk. Ph.D. thesis, University of London.

Avery, B. W. & Bascomb, C. L. 1982 Soil Survey laboratory methods. *Soil Surv. tech. Monogr.* **6**, 1–83.

Avery, B. W. & Bullock, P. 1977 Mineralogy of clayey soils in relation to soil classification. *Soil Surv. tech. Monogr.* **10**, 1–64.

Bertouille, H. 1972 Effet du gel sur les sols fin. *Revue Géomorph. dyn.* **11**, 71–84.

Black, R. F. 1976 Periglacial features indicative of permafrost: ice and soil wedges. *Quat. Res.* **6**, 3–26.

Blume, H. P. & Schwertmann, U. 1969 Genetic evaluation of profile distribution of aluminium, iron and manganese oxides. *Proc. Soil Sci. Soc. Am.* **33**, 438–444.

Bouma, J., Pons, L. J. & Van Schuylenburgh, J. 1968 On soil genesis in temperate humid climate: VI. The formation of a glossudalf in loess (silt loam). *Neth. J. agric. Sci.* **16**, 58–70.

Brewer, R. 1972 The basis of interpretation of soil micromorphological data. *Geoderma* **8**, 81–84.

Brewer, R. 1976 *Fabric and mineral analysis of soils.* New York: Krieger.

Brown, G. & Wood, I. G. 1985 Estimation of iron oxides in soil clays by profile refinement combined with differential x-ray diffraction. *Clay Miner.* **20**, 15–28.

Bullock, P. & Murphy, C. P. 1979 Evolution of a paleoargillic brown earth (Paleudalf) from Oxfordshire, England. *Geoderma* **22**, 225–253.

Bullock, P., Federoff, N., Jongerius, A., Stoops, G. & Tursina, T. 1985 *Handbook for soil thin section description.* Wolverhampton: Wayne Research.

Castellet, J. T. & FitzPatrick, E. A. 1974 Clay cutan and matrix disruption in a soil from central Spain. In *Soil microscopy* (ed. G. K. Rutherford), pp. 632–641. Kingston: Limestone Press.

Chartres, C. J. 1980 A Quaternary soil sequence in the Kennet Valley, central southern England. *Geoderma* **23**, 125–146.

Corte, A. E. 1961 The frost behaviour of soils: laboratory and field data for a new concept. Part 1: vertical sorting. *U.S. Army Cold Regions Res. & Eng. Lab. Res. Rept.* **85**, 1–22.

Dumanski, J. 1964 A micromorphological study of eluvial horizons. M.Sc. Thesis, University of Saskatchewan.

Dumanski, J. & St. Arnaud, R. J. 1966 A micropedological study of eluvial horizons. *Can. J. Soil Sci.* **46**, 287–293.

Federoff, N. 1974 Classification of accumulations of translocated particles. In *Soil microscopy* (ed. G. K. Rutherford), pp. 695–713. Kingston: Limestone Press.

Federoff, N. & Goldberg, P. 1982 Comparative micromorphology of two late Pleistocene paleosols (in the Paris Basin). *Catena* **9**, 227–251.

FitzPatrick, E. A. 1971 *Pedology, a systematic approach to soil science.* Edinburgh: Oliver & Boyd.

FitzPatrick, E. A. 1974 Cryons and isons. *Proc. N. Engl. Soils Discuss. Group* **11**, 31–43.

French, H. M. 1976 *The periglacial environment.* London: Longman.

Gladfelter, B. G. 1972 Cold climate features in the vicinity of Clacton-on-Sea, Essex, (England). *Quaternaria* **16**, 121–135.

Harris, C. 1985 Geomorphological applications of soil micromorphology with particular reference to periglacial sediments and processes. In *Geomorphology and soils* (ed. K. S. Richards, R. S. Arnett & S. Ellis), pp. 219–232. London: George Allen & Unwin.

Harris, C. & Ellis, S. 1980 Micromorphology of soils in soliflucted materials, Okstinden, northern Norway. *Geoderma* **23**, 11–29.

Hey, R. W. 1980 Equivalents of the Westland Green Gravels in Essex and East Anglia. *Proc. geol. Ass.* **91**, 279–290.

Hodgson, J. M. 1976 Soil survey field handbook. *Soil Surv. Tech. Monogr.* **5**, 1–99.

Kemp, R. A. 1985*a* The Valley Farm Soil in southern East Anglia. In *Soils and Quaternary landscape evolution* (ed. J. Boardman), pp. 179–196. Chichester: Wiley.

Kemp, R. A. 1985*b* Soil micromorphology and the Quaternary. *Quat. Res. Ass. tech. Guide* **2**, 1–80.

Kemp, R. A. 1985*c* The cause of redness in some buried and non-buried soils in eastern England. *J. Soil Sci.* **36**, 329–334.

Mackay, J. R. & Matthews, J. V. 1983 Pleistocene ice and sand wedges, Hooper Island, North-west Territories. *Can. J. Earth Sci.* **20**, 1087–1097.

McKeague, J. A. & Day, J. H. 1966 Dithionite- and oxalate-extractable Fe and Al as aids in differentiating various classes of soils. *Can. J. Soil Sci.* **46**, 13–22.

McKeague, J. A., Acton, C. J. & Dumanski, J. 1974 Studies of soil micromorphology in Canada. In *Soil microscopy* (ed. G. K. Rutherford), pp. 84–100. Kingston: Limestone Press.

McMillan, N. J. & Mitchell, J. 1953 A microscopic study of platy and concretionary structures in certain Saskatchewan soils. *Can. J. agric. Sci.* **33**, 178–183.

Mermut, A. & St. Arnaud, R. J. 1981 Microband fabric in seasonally frozen soils. *Proc. Soil Sci. Soc. Am.* **45**, 578–586.

Moore, T. R. 1973 The distribution of iron, manganese and aluminium in some soils from northeast Scotland. *J. Soil Sci.* **24**, 162–171.

Mucher, H. J., Carballas, T., Guitián Ojea, F., Jungerius, P. D., Kroonenburg, S. B. & Villar, M. C. 1972 Micromorphological analysis of effects of alternating phases of landscape stability and instability on two soil profiles in Galicia, N.W. Spain. *Geoderma* **8**, 241–266.

Murphy, C. P. & Kemp, R. A. 1984 Overestimation of clay and underestimation of pores in soil thin sections. *J. Soil Sci.* **35**, 481–495.

Pawluk, S. & Brewer, R. 1975 Micromorphological and analytical characteristics of some soils from Devon and King Christian Islands, NWT. *Can. J. Soil Sci.* **55**, 349–361.

Rhoton, F. E., Bigham, J. M., Norton, L. D. & Smeck, N. E. 1981 Contribution of magnetite to oxalate-extractable iron in soils and sediments from the Maumee River Basin of Ohio. *Proc. Soil Sci. Soc. Am.* **45**, 645–649.

Romans, J. C. C. & Robertson, L. 1974 Some aspects of the genesis of alpine and upland soils in the British Isles. In *Soil microscopy* (ed. G. K. Rutherford), pp. 498–510. Kingston: Limestone Press.

Romans, J. C. C., Robertson, L. & Dent, D. L. 1980 The micromorphology of young soils from south-east Iceland. *Geogr. Annlr.* **62** A, 93–103.

Romans, J. C. C., Stevens, J. H. & Robertson, L. 1966 Alpine soils of north-east Scotland. *J. Soil Sci.* **17**, 184–199.

Rose, J., Allen, P. & Hey, R. W. 1976 Middle Pleistocene stratigraphy in southern East Anglia. *Nature, Lond.* **263**, 492–494.

Rose, J., Allen, P., Kemp, R. A., Whiteman, C. A. & Owen, N. 1985 The early Anglian Barham Soil of Eastern England. In *Soils and Quaternary landscape evolution* (ed. J. Boardman), pp. 197–229. Chichester: Wiley.

Schwertmann, U. & Taylor, R. M. 1977 Iron oxides. In *Minerals in soil environments* (ed. J. B. Dixon & S. B. Weed), pp. 145–180. Madison: Soil Science Society of America.

Torrent, J., Nettleton, W. D. & Borst, G. 1980 Clay illuviation and lamella formation in a Psammentic Haploxeralf in southern California. *Proc. Soil Sci. Soc. Am.* **44**, 363–369.

Van Vliet-Lanoe, B. 1976 Traces de ségrégation de glace en lentilles associées aux sols et phénomènes periglaciaires fossiles. *Biul. peryglac.* **26**, 41–55.

Van Vliet-Lanoe, B. 1982 Structures et microstructures associées à la formation de glace de ségrégation: leur conséquences. *Proc. 4th Can. Permafrost Conf.*, 116–122.

Van Vliet-Lanoe, B. 1985 Frost effects in soils. In *Soils and Quaternary landscape evolution* (ed. J. Boardman), pp. 117–158. Chichester: Wiley.

Walker, T. R., Waugh, B. & Grone, A. J. 1978 Diagenesis in first cycle desert alluvium of Cenozoic age, southwest United States and northwestern Mexico. *Bull. geol. Soc. Am.* **89**, 19–32.

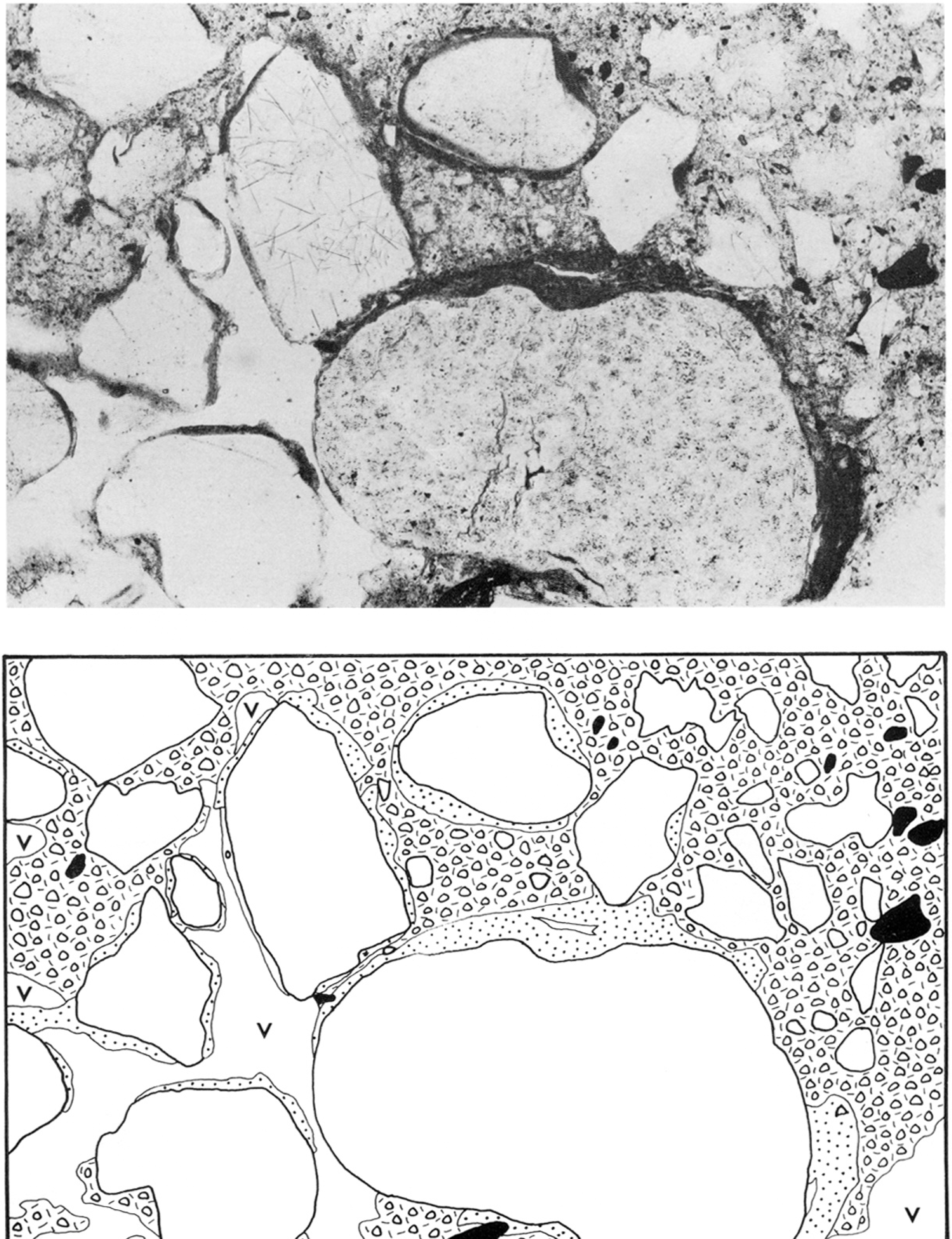

FIGURE 4. Photomicrograph (top) and interpretative diagram (bottom) of sand grains, coated with impure clay and embedded within groundmass in thin section 1b. Plane polarized light (PPL); horizontal frame length (HFL) = 1.3 mm.

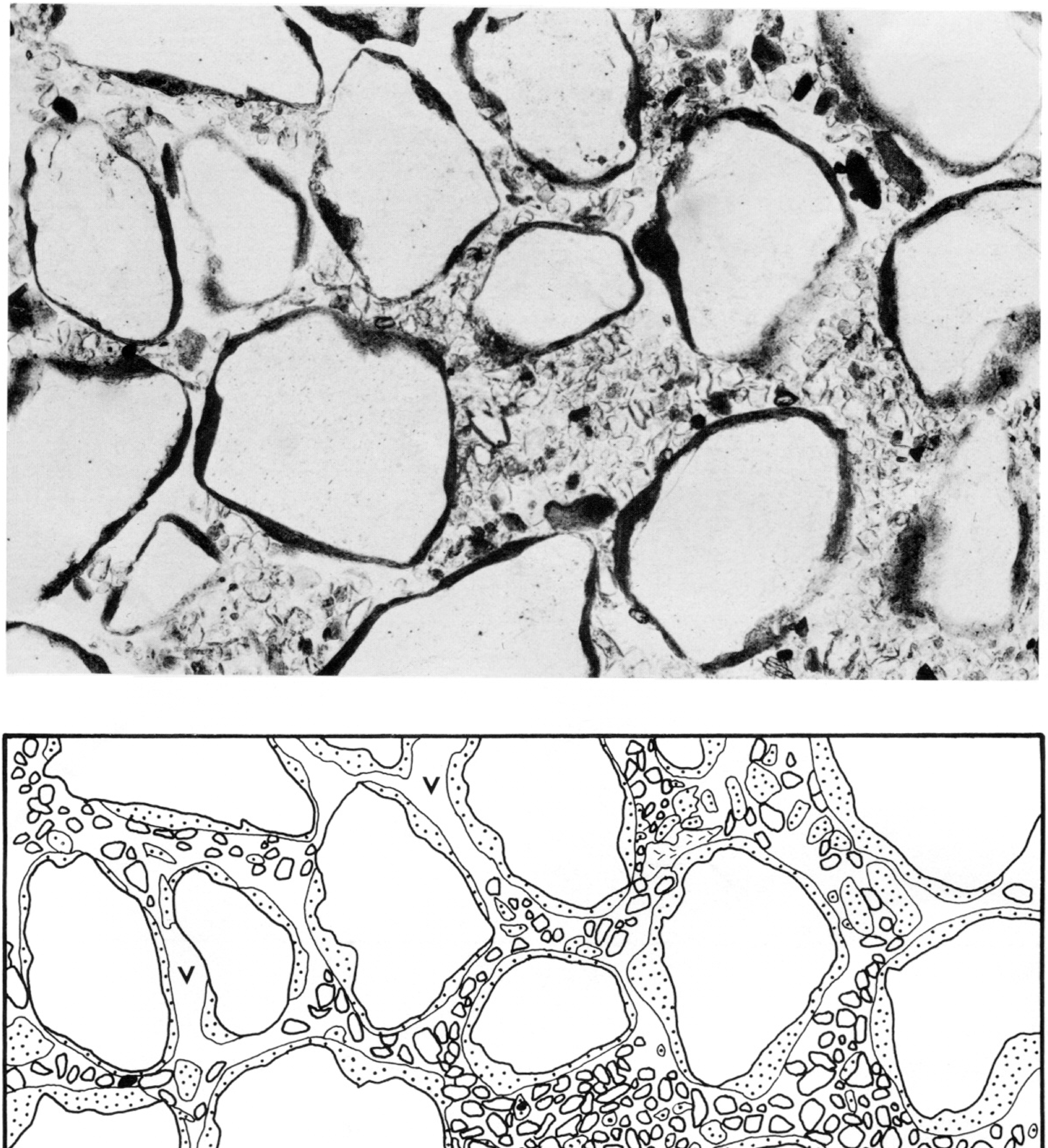

FIGURE 5. Photomicrograph (top) and interpretative diagram (bottom) of sand grains, coated with impure clay and embedded within clusters of silt-size mineral grains and fragmented clay coatings in thin section 1c. PPL; HFL = 1.3 mm (key as for figure 4b).

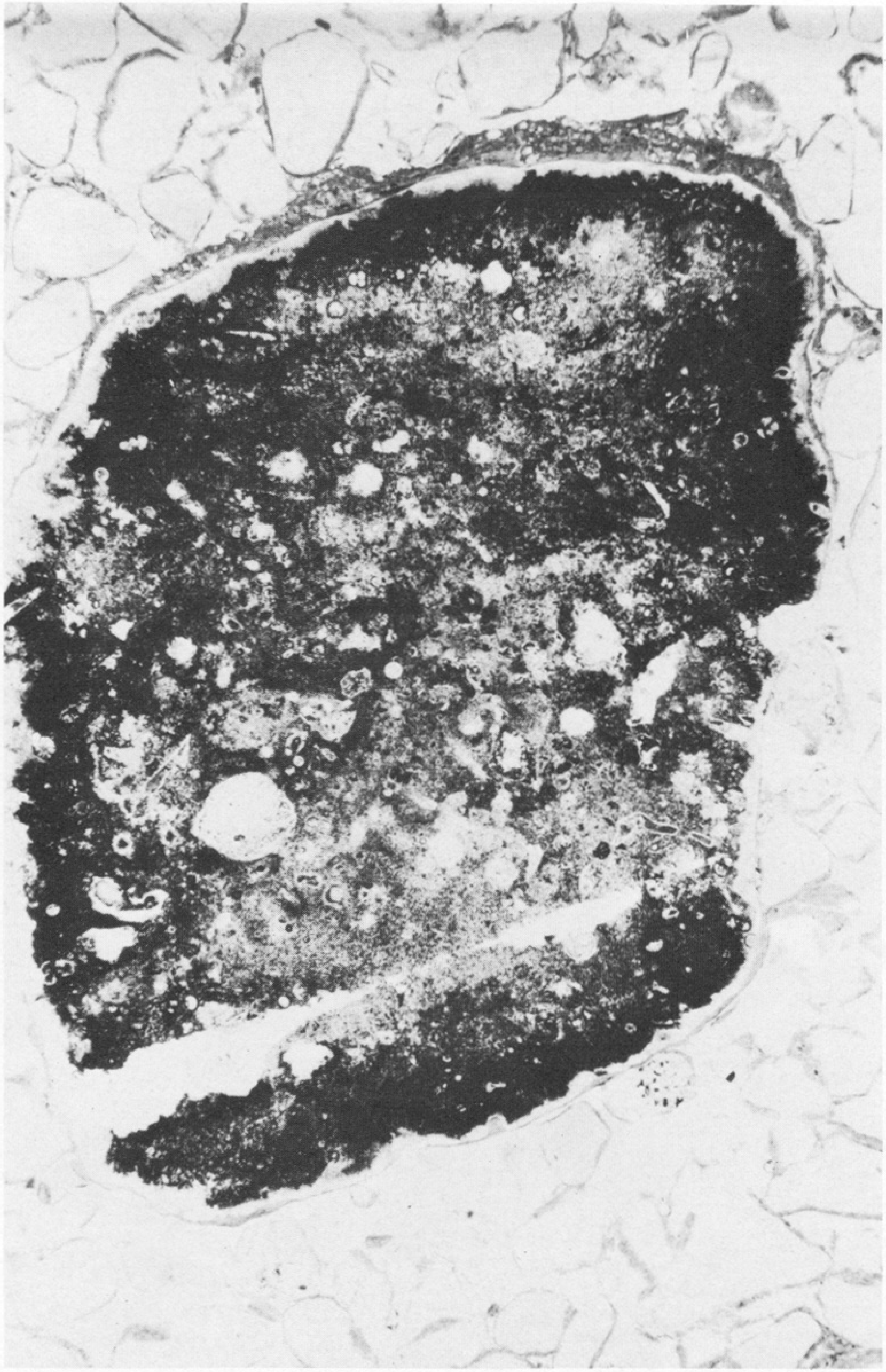

FIGURE 6. Photomicrograph of a silty clay capping upon a chert clast in thin section 1c. PPL; horizontal frame width (HFW) = 3.4 mm.

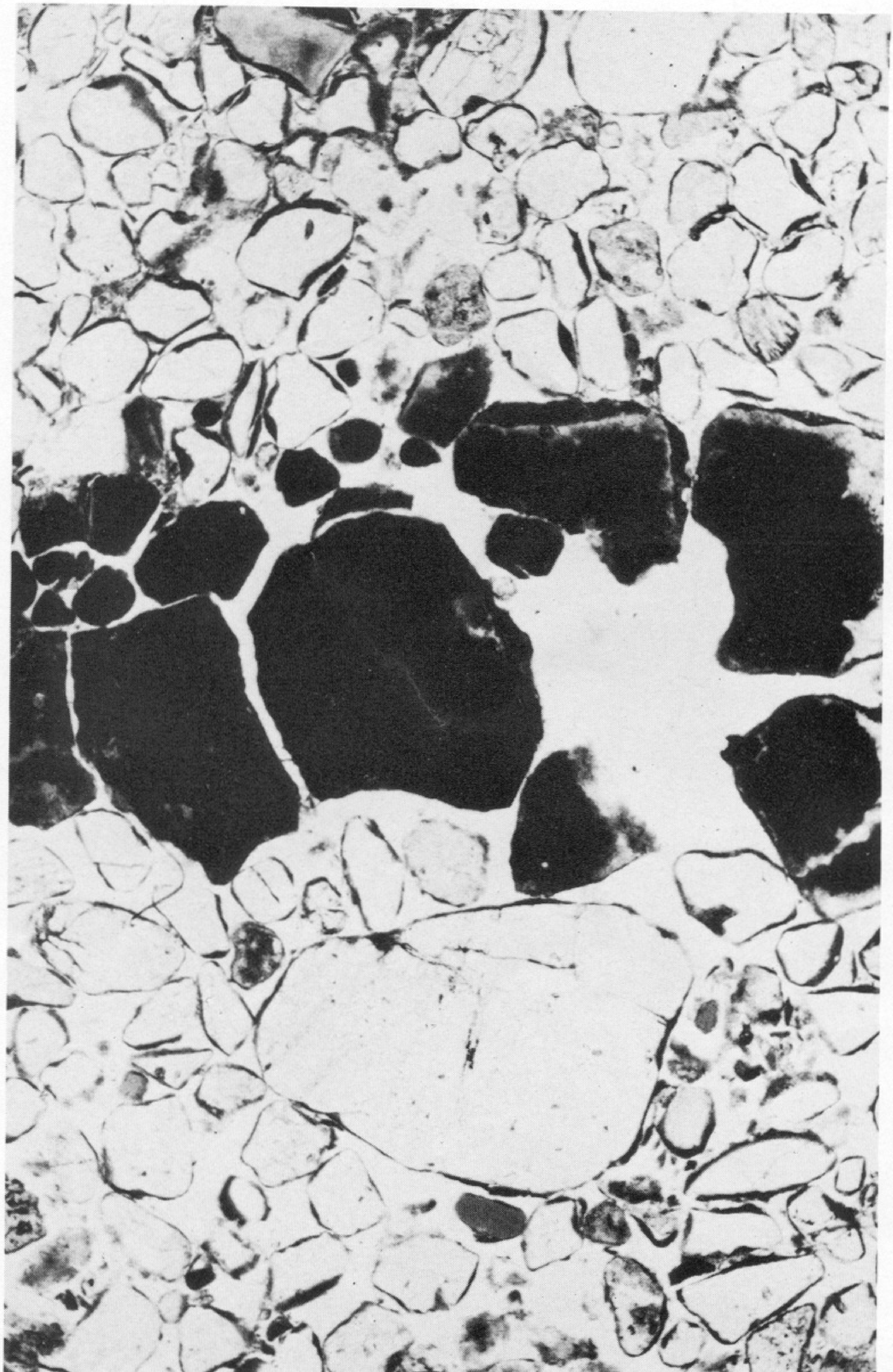

FIGURE 7. Photomicrograph of a chert clast fractured into conjoinable fragments in thin section 1c. PPL; HFW = 3.4 mm.

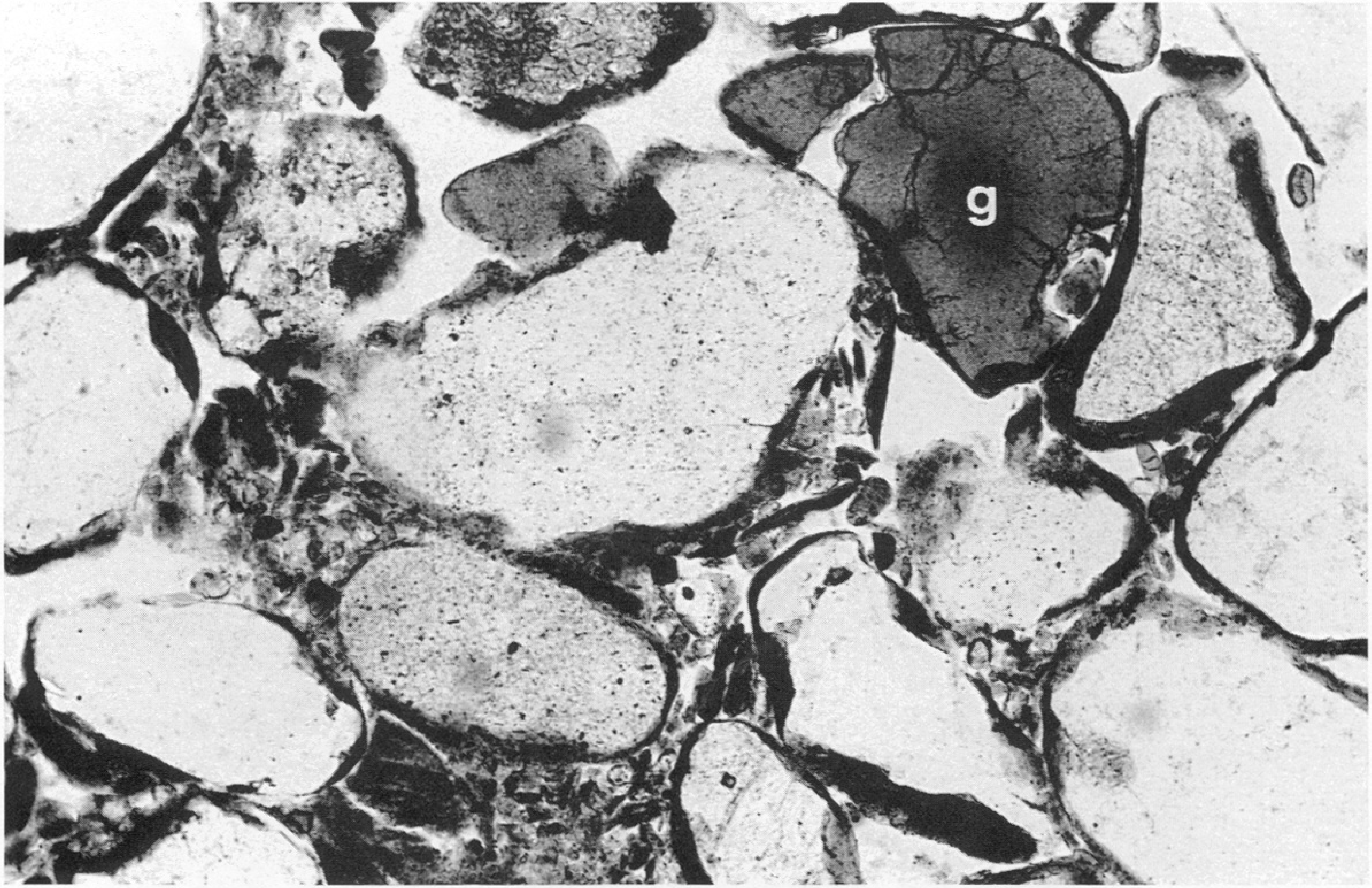

FIGURE 8. Photomicrograph showing a weathered (fragmented) glauconite grain (g) in thin section 2d. PPL; HFL = 1.3 mm.

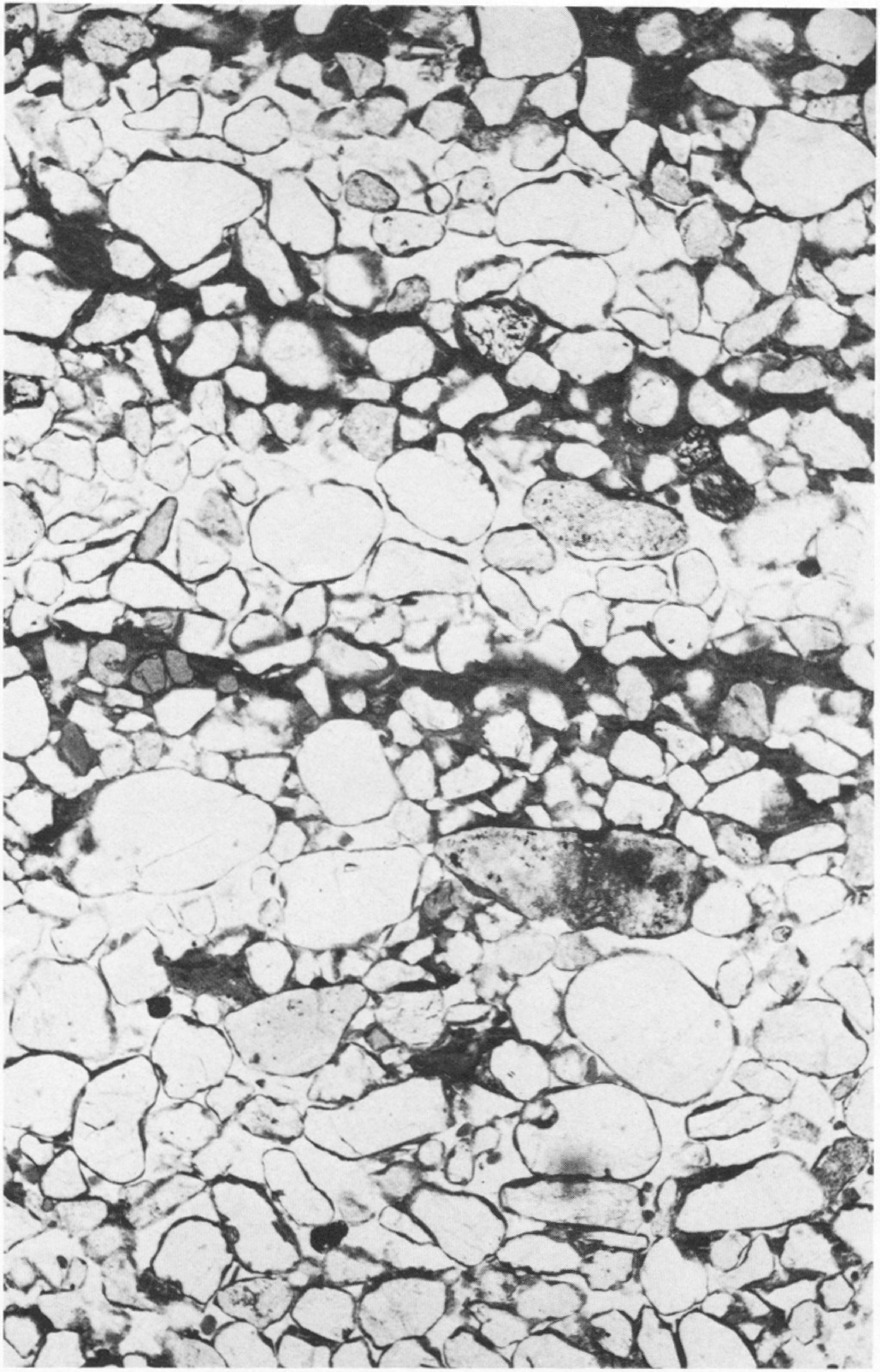

FIGURE 9. Photomicrograph of duplex textural lamellae a-features in thin section 2e. PPL; HFW = 3.4 mm.

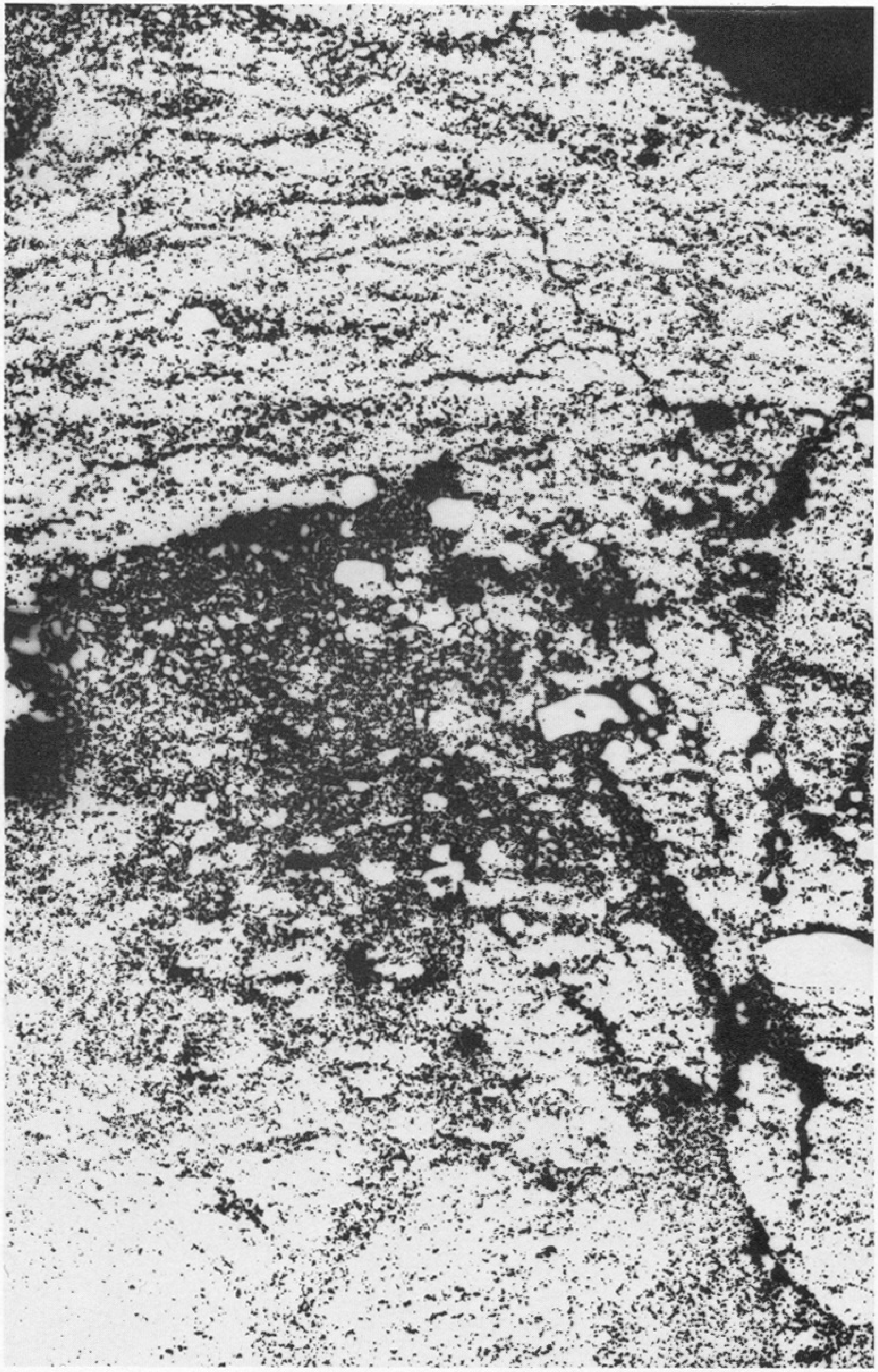

FIGURE 10. Contact print of impregnated block adjacent to surface used for thin section 2e, which shows platy structure (black areas are voids). HFW = 5 cm.

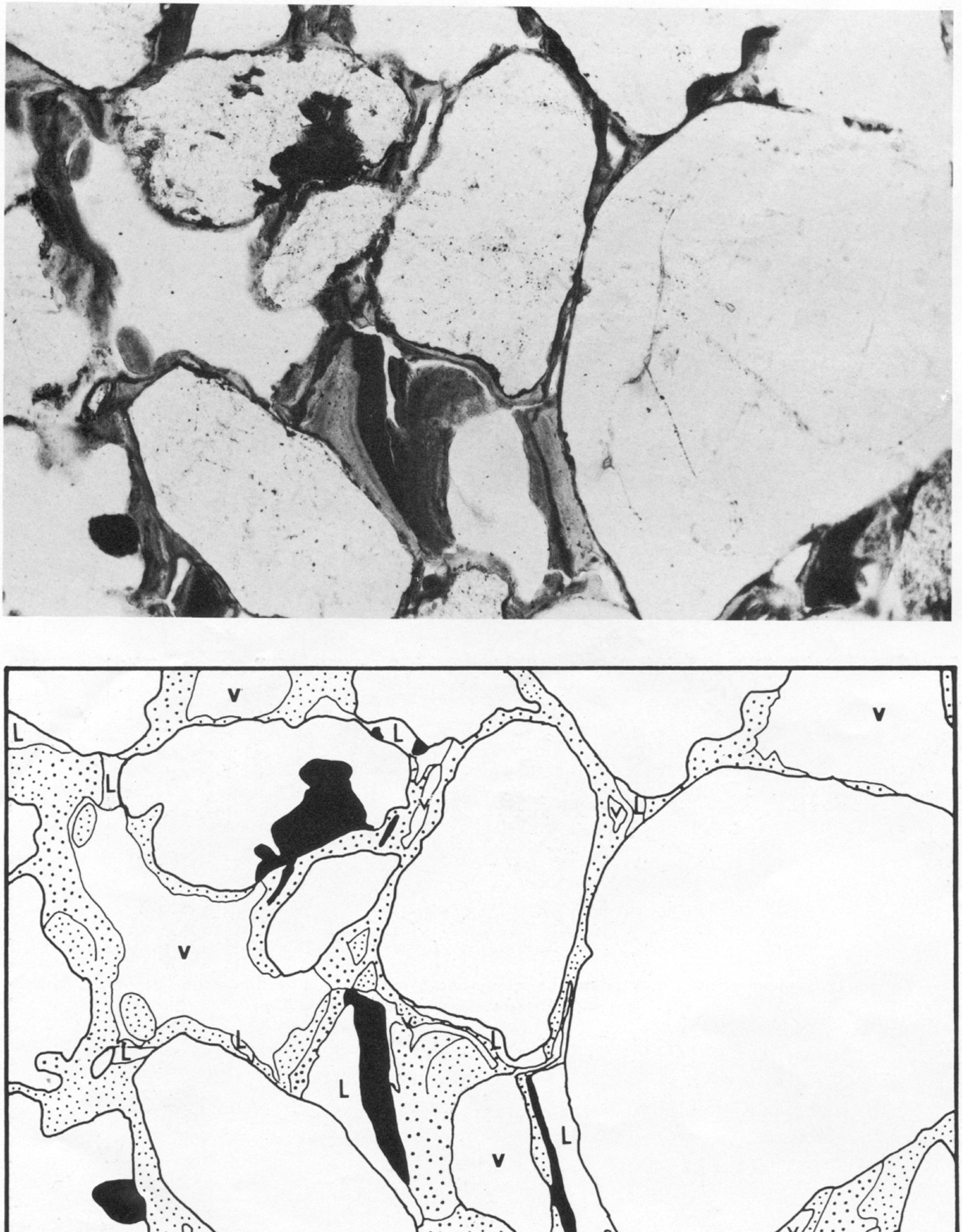

FIGURE 11. Photomicrograph (top) and interpretative diagram (bottom) of limpid clay coatings around sand grains which are postdated by complex speckled–impure clay coatings in thin section 1e. PPL; HFL = 1.3 mm (key as for figure 4*b*).

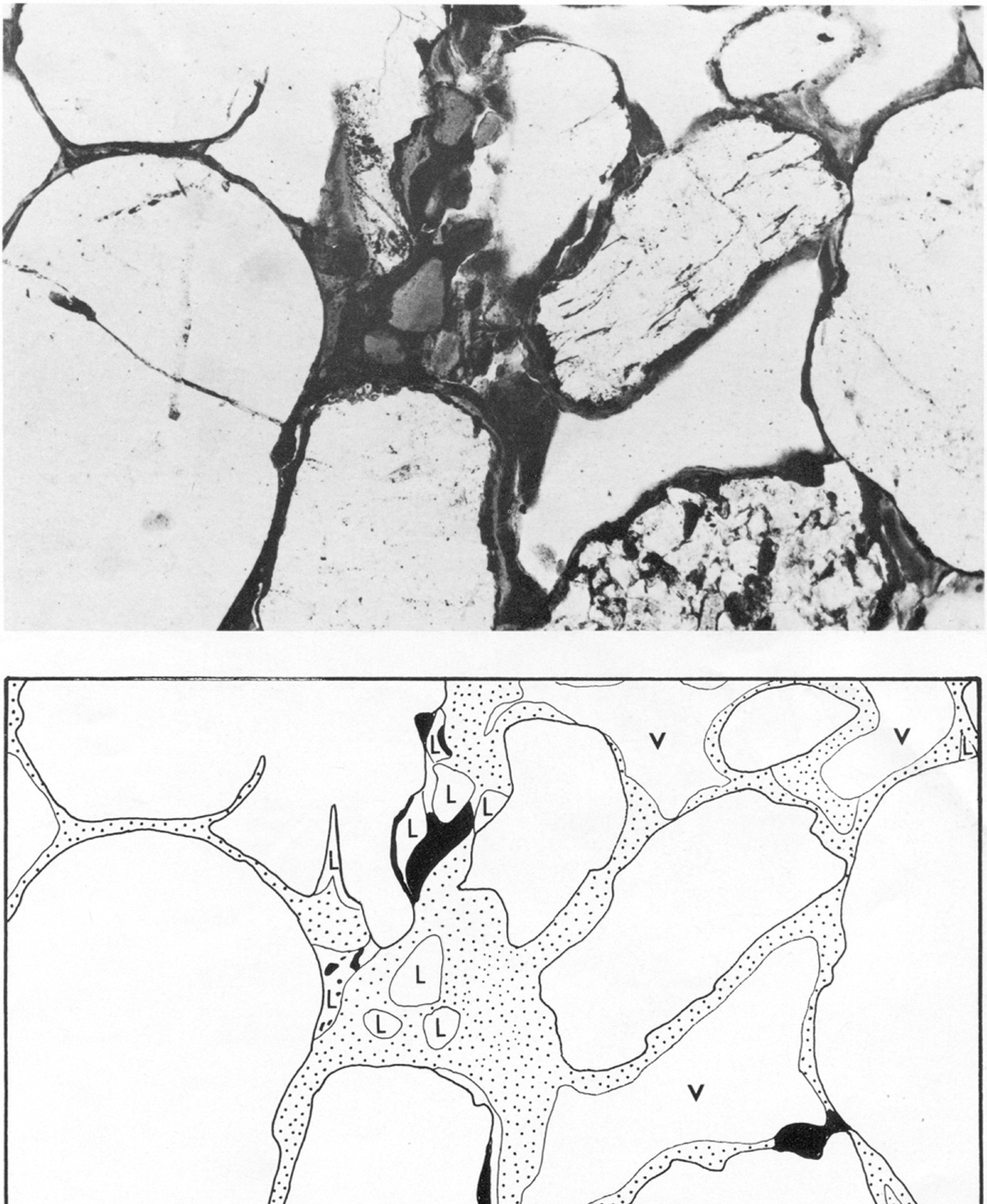

Figure 12. Photomicrograph (top) and interpretive diagram (bottom) of limpid clay coatings around sand grains with adjacent fragmented coatings of similar composition embedded within speckled–impure clay coatings in thin section 1e. PPL; HFL = 1.3 mm (key as for figure 4*b*).

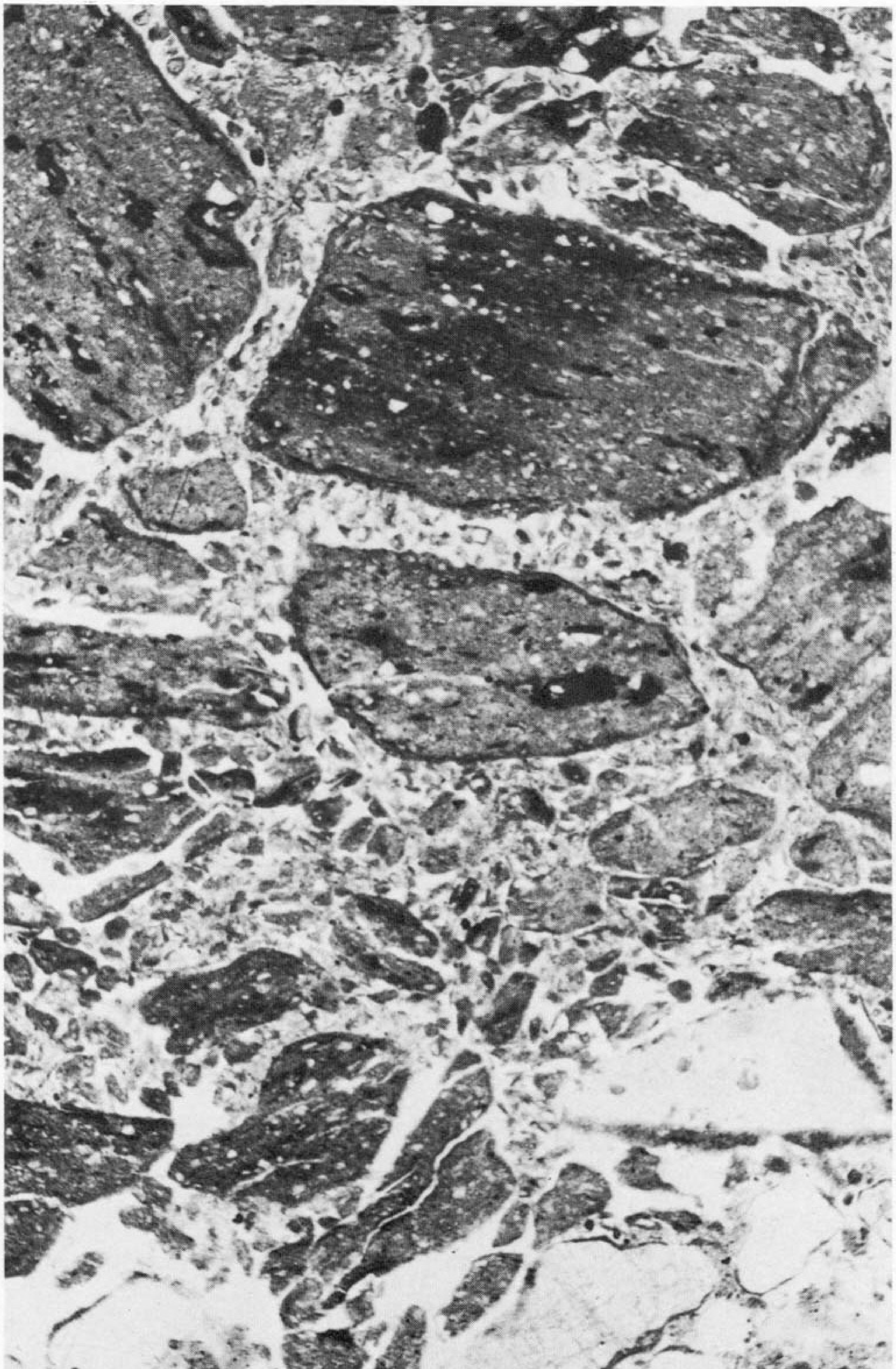

FIGURE 13. Photomicrograph of fragmented micaceous, silty clay lenses in thin section 2d. PPL; HFW = 3.4 mm.